Figure 4. Expression of ORP150 suppresses Purkinje cell death during cerebellar development. A–O, ORP150 $^{/-}$, ORP150 $^{/ /}$, or Tg ORP150 mice were perfusion fixed at P1, P4, P6, P10, and P30 and stained with antibody to calbidin D$_{28k}$ only (Calb; E, J, O) or double-stained by TUNEL assay and antibody to calbindin D$_{28k}$ (A–C, F–H, K–M), or antibodies to calbindin D$_{28k}$ and activated caspase-3 (Casp3; D, I, N). Scale bars, 100 μm; images are representative of six experiments. P, The percentage of TUNEL-positive nuclei colocalized with calbindin D$_{28k}$-positive cells in ORP150 $^{+/-}$ (open bars), ORP150 $^{+/-}$ (shaded bars), or Tg ORP150 (filled bars) mice was determined in samples prepared 6 and 12 d after birth. Q, The percentage of cellular profiles positive for both activated caspase-3 and calbindin D$_{28k}$ in ORP150 $^{+/-}$ (open bars), ORP150 $^{+/+}$ (shaded bars), or Tg ORP150 (filled bars) mice was determined in samples prepared 4 and 12 d after birth. **p < 0.01; *p < 0.05, compared with non-Tg littermates (n = 6 per time point). R, The population of Purkinje cells (calbindin D$_{28k}$-positive cells) was counted in the cerebellar hemisphere of Tg ORP150 (filled bars) and ORP150 $^{+/-}$ (open bars) mice at 4, 10, 20, and 30 d after birth. Values are expressed as fold increase or decrease compared with non-Tg littermates; n = 6 per time point. **p < 0.01, nonpaired t test compared with non-Tg (wild-type) littermates.

2001; Chena et al., 2002). In the open-field test (Fig. 6A), ORP150 $^{+/-}$ mice displayed performance identical to that of ORP150 $^{/ /}$ animals. In contrast, motor coordination, assessed by the rotor rod test (Fig. 6B), showed significant impairment in Tg ORP150 mice. These data suggest that overexpression of ORP150, although enhancing the viability of Purkinje cells in early development and increasing their numbers in adult animals, ultimately caused cerebellar dysfunction. There were no differences in performance of ORP150 $^{+/-}$ and ORP150 $^{+/+}$ mice (data not shown).

Normal cerebellar synaptic function in ORP150 mutant mice
To probe the mechanism underlying cerebellar dysfunction in mutant mice, we examined the electrophysiological properties of Purkinje cells using whole-cell recordings in cerebellar slices. We first compared passive membrane properties of Purkinje cells by recording membrane currents in response to hyperpolarizing voltage steps from the holding potential of −70 to −80 mV. As reported previously (Llano et al., 1991), the decay of the current was biphasic and could be described by the sum of two exponen-

tials (data not shown). From their time constants, we calculated several parameters representing passive properties of Purkinje cells on the basis of the model equivalent circuit of Purkinje cells described by Llano et al. (1991) (Table 1). This model distinguishes two regions in the Purkinje cell. Region 1 represents the soma and the main proximal dendrite, and region 2 represents the main part of dendritic tree. The lumped membrane capacitance of regions 1 and 2 were calculated as C1 and C2, respectively. R1 represents the pipette access resistance. Region 2 is linked to region 1 by resistor R2, which represents the lumped resistance between the main proximal dendrite and each membrane region of the distal dendrites. R3 represents the lumped resistance of the dendritic tree of Purkinje cells. With respect to these parameters, we found no significant differences among ORP150 $^{-/+}$, ORP150 $^{+/+}$, and Tg ORP150 mice (Table 1). These results suggest that the size of the soma and the main proximal dendrite and the extent of the dendritic tree are similar in these three strains of mice.

Purkinje cells receive two distinct excitatory inputs: parallel fibers (the axons of granule cells) and climbing fibers (the axons
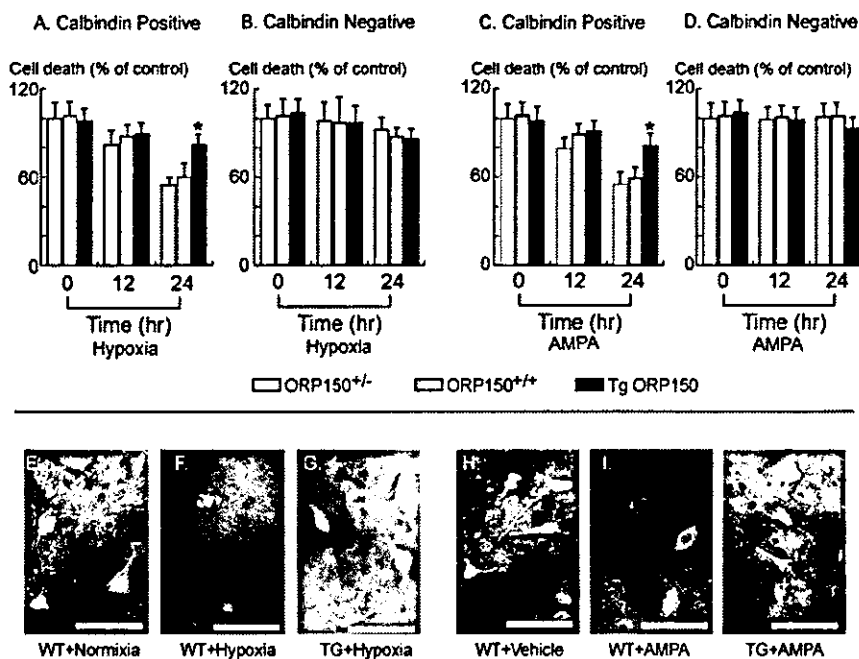
Figure 5. Effect of ORP150 on Purkinje cell death *in vitro*. *A–D*, Purkinje cells were prepared from ORP150 $^{+/-}$ (open bars), ORP150 $^{-/+}$ (shaded bars), or Tg ORP150 (filled bars) mice within 1 d after birth. Cells were then incubated in astrocyte-conditioned medium, as described in Materials and Methods, for 10 d and exposed to hypoxia (*A, B*) for 0–24 hr. Viability of Purkinje cells (*A*) and non-Purkinje cells (*B*) was then assessed at the indicated time points, as described in Materials and Methods. Purkinje cells (*C*) and non-Purkinje cells (*D*) were also exposed to AMPA (30 μM) under normoxic conditions. At the indicated time points, cell viability was assessed. Values are expressed as percent cell death compared with the viability of the untreated cultures. *$p < 0.01$, compared with wild-type cultures by multiple-contrast analysis followed by two-way ANOVA. *E–J*, Representative images of immunostaining of cultures from wild-type (WT; non-Tg) animals under controlled conditions, neurons from WT animals exposed to hypoxia (*F*) or AMPA (*I*), or neurons from Tg ORP150 mice (TG) exposed to hypoxia (*G*) or AMPA (*J*). Incubation of cultures under hypoxic conditions (*E, F*) or exposure to AMPA (30 μM; *H–J*) was for 24 hr. Scale bars, 100 μm. Images are representative of six experiments.

of the inferior olivary neurons) (Ito, 1984). Individual Purkinje cells are innervated by multiple climbing fibers initially during early development, but supernumerary climbing fibers are pruned subsequently, and most Purkinje cells become monoinnervated by the third postnatal week (Crepel et al., 1981; Mariani and Changeux, 1981a,b). Several knock-out mice show abnormal retention of multiple climbing fiber innervation and impairment of motor coordination (Kano et al., 1995, 1997). Thus, we examined whether multiple climbing fiber innervation persists in the ORP 150 mutant mice. We estimated the number of climbing fibers innervating each Purkinje cell by electrophysiological examination (Kano et al., 1995, 1997). When a climbing fiber was stimulated, an EPSC was elicited in an all-or-none manner in the majority of Purkinje cells (Fig. 6*A*), indicating that such Purkinje cells were innervated by single climbing fibers. In some Purkinje cells, more than one discrete climbing fiber-mediated EPSC (CF-EPSC) could be elicited when the stimulating electrode was moved systematically by 20 μm steps and the stimulus intensity was increased gradually at each stimulation site. The number of climbing fibers innervating the Purkinje cell was estimated by counting the number of discrete CF-EPSC steps. The summary graph in Figure 6*B* indicates that frequency distribution of Purkinje cells in terms of the number of CF-EPSC steps (Fig. 6*A,B*) showed no significant difference between the three genetically manipulated mice ($p > 0.05$, χ^2 test). These results suggest that developmental elimination of surplus climbing fibers is normal in these mice. We then examined basic electrophysiological properties of EPSCs by stimulating climbing fibers and parallel fibers.

We first examined the kinetics of CF-EPSCs. The 10–90% rise times, decay time constants, and amplitudes were similar among the three strains of mice (data not shown). We then examined short-term plasticity of climbing fiber and parallel fiber synapses. In normal external calcium concentration (2 mM), CF-EPSCs display depression, whereas parallel fiber-mediated EPSCs (PF-EPSCs) undergo facilitation, to the pair of stimuli (Konnerth et al., 1990; Aiba et al., 1994). The paired pulse depression of CF-EPSCs (pulse interval, 10–3000 msec) and the paired pulse facilitation of PF-EPSCs (pulse interval, 10–300 msec) were similar among the three strains of mice (data not shown). These results indicate that basic properties of CF- and PF-EPSCs are normal in these mice.

Discussion

Integral to development of the central nervous system is loss of a large number of neurons through "naturally occurring cell death," by mechanisms that remain to be elucidated (Calabrese et al., 2002). Morphological evidence suggests that such cell death often displays characteristics typical of apoptosis as a final common pathway. However, the key issue is to identify endogenous triggers and breaks on this system that enable selected neuronal populations to survive and to form complex synaptic networks, whereas others are eliminated. Expression of molecular chaperones in developing brain, such as ORP150, suggests the presence of ongoing neuronal stress probably attributable, in part, to perturbations in the local environment. ORP150 was first identified as a stress protein in astrocytes exposed to severe hypoxia (Kuwabara et al., 1996). Because ORP150 is localized to the ER and expressed in response to stress, upregulation of Purkinje cell ORP150 suggests the presence of an ongoing stress response during cerebellar development.

Molecular chaperones are abundant, well conserved proteins essential for maintaining cellular function (Wynn et al., 1994). Environmental stress focused on the ER (termed ER stress) causes a proteotoxic insult: immature proteins accumulate in the ER; conformational changes occur (Patil and Walter, 2001); and induction of molecular chaperones is the result. The protective role of chaperones is crucial for cell survival and repair in response to environmental challenge. In this context, we have previously demonstrated that ORP150 has neurotrophic properties in a range of settings, including ischemia-induced cell death (Tamatani et al., 2001), excitotoxicity (Kitao et al., 2001), and delayed neuronal cell death (Miyazaki et al., 2002). In this article, we have extended this concept by showing that expression of ORP150 in Purkinje cells decreases their vulnerability to hypoxic and excitotoxic stress and enhances their survival during development *in vivo*.

Certain neuronal populations display selective vulnerability to toxic insults, potentially resulting in loss of those cells. Purkinje cells, in particular among cerebellar neurons, are suscepti-

A.

B.
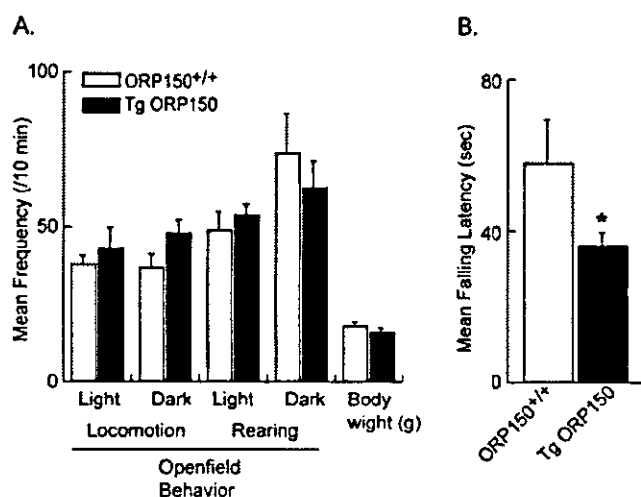
Figure 6. Behavioral analysis of Tg ORP150 mice. Open-field activity (*A*) and rotor rod behavior (*B*) were assessed in non-Tg littermates (ORP150 $^{+/-}$; shaded bars) and Tg ORP150 mice (filled bars). *A*, Open-field performance was examined using an acrylic box as described in Materials and Methods. The total number of crossings across the two infrared rays attached 2 cm above the floor on each *x* and *y* bank was counted during first 10 min (with light on; Light) and the following 10 min (with the light off; Dark) as traveling behavior of the animal (Locomotion). The total number of crossings across the 12 infrared rays attached 5 cm above the floor on the *x* bank was counted during the first 10 min (Light) and the following 10 min (Dark) as rearing behavior of the animal (Rearing). Values are expressed as mean frequency of each activity in each period. Body weights of phenotype mice are also shown at the right. *B*, Motor coordination was evaluated by the mean of falling latency from the rotor rod using an acceleration protocol (2.5, 5, and 7.5 rpm followed by 10 rpm for 30 sec each). Values are mean ± SE. ORP150 $^{+/+}$, *n* = 9 for each condition; Tg ORP150, *n* = 6 for each condition. *p < 0.05, Student's *t* test.

ble to ischemic stress (Sieber et al., 1995; Yoshida et al., 2002), as well as other neurodegenerative-associated conditions (Dove et al., 2000). A likely final common pathway for such toxicity is elevation of free $[Ca^{2+}]i$. Increased $[Ca^{2+}]i$ is associated with a number of cytotoxic events, including chronic ethanol intoxication (Netzeband et al., 1999), diseases characterized by accumulation of proteins with polyglutamine repeats (Clark and Orr, 2000), and traumatic brain injury (Netzeband et al., 1999). Molecular chaperones in the ER have the capacity to function as a buffer system to suppress elevated $[Ca^{2+}]i$ by the maintaining the complex metabolic and biosynthetic properties of this organelle (Yu et al., 1999). In this context, we have demonstrated that ORP150 also suppresses elevations of $[Ca^{2+}]i$ in cultured hippocampal neurons exposed to excitatory amino acids (Kitao et al., 2001). Our preliminary observations reveal expression of ORP150 in Purkinje cells in the setting of human stroke and a primate model of experimental brain ischemia. Taken together, these observations further support the concept that expression of ORP150 in Purkinje cells during development (P4–P8; Figs. 1, 2) is indicative of the presence of environmental stress, potentially ischemic, excitotoxic, or both (see below).

Our current results demonstrate selective upregulation of

ORP150 in the developing cerebellum, whereas levels of other molecular chaperones, such as GRP78, remain unchanged. From an evolutionary point of view, these two stress proteins (ORP150 and GRP78) have overlapping functions in yeast. Null mutant strains of lumenal Hsp seventy (LHS)1, the yeast homolog of ORP150, display "compensatory" upregulation of Kar2p, the yeast homolog of GRP78. Although each gene alone is not essential for yeast viability, lethality is observed when inactivating mutations are introduced into both Kar2p and LHS1 (Craven et al., 1996). In contrast, our previous study demonstrated embryonic lethality in homozygous ORP150 $^{-/-}$ embryos (in which the ORP150 gene had been deleted by homologous recombination and replaced by an inactive, truncated form). Thus, it appears that properties of ORP150 and GRP78 have diverged over time; the function of ORP150 cannot be complemented by increased expression of GRP78, and ORP150 appears to be essential for survival in mammalian embryogenesis (Craven et al., 1996). A similar critical role for the HSP47, another molecular chaperone in the ER, in embryonic development has been shown; a genomic mutant of HSP47 also results in embryonic lethality (Nagai et al., 2000).

Mechanisms underlying the vulnerability of cerebellar Purkinje cells to environmental stress remain to be clarified. Cell differentiation and synaptogenesis in cerebellum come in different waves depending on the neuronal populations and afferents and are highly interactive mutually (Altman and Bayer, 1997). In rats, the first postnatal wave comes at P4, characterized with rapid growth in cortex. Most PCs were already multiply innervated by CFs as early as 3 d. The multiple innervation culminated on P5, which rapidly regressed later on (Zhao et al., 1998; Miranda-Contreras et al., 1999). Our results demonstrate increased Purkinje cell death at P4–P6. Though the synaptic formation of climbing fibers from the inferior olive are still immature and confined in somatic regions (Altman and Bayer, 1997), strong immunostaining of glutamate receptor subunits 2 and 3 could be observed at postnatal days 1–3 within Purkinje cell bodies and primary dendrites (Bergmann et al., 1996; Hafidi and Hillman, 1997). At this stage of development, vesicular glutamate transporter is expressed in terminals around PC soma at P1–P10 (Miyazaki T et al., 2003). Because this transporter mainly mediates the filling of cytoplasmic glutamate into synaptic vesicles in terminals, its expression indicates that glutamate release at CF → PC synapses is functional from the molecular point of view, suggesting that polyinnervation of CFs during the first postnatal week could be glutamate stress to developing PCs. A certain extent of Purkinje cell death at this point in development appears to be essential for optimal cerebellar function. Although synaptic properties of Purkinje cells in Tg ORP150 mice appeared normal (Fig. 7), and the number of these neurons was increased (Fig. 4), cerebellar function was clearly suboptimal (Fig. 6). Thus, it is possible that the agility with which certain neuronal populations mount an ER stress response may have important implications for their vulnerability to a range of environmental perturbations.

Table 1. Passive membrane properties of PCs

Mice	C1 (pF)	C2 (pF)	R1 (MΩ)	R2 (MΩ)	Rm (R3) (MΩ)	n
ORP150 $^{-/+}$	162.2 ± 87.4	847.6 ± 203.4	6.4 ± 1.1	9.0 ± 2.8	181.5 ± 70.6	16
ORP150 $^{-/+}$	154.8 ± 68.7	870.7 ± 230.9	6.1 ± 0.9	8.0 ± 2.5	162.7 ± 70.8	25
Tg ORP150	171.6 ± 78.1	854.0 ± 120.9	6.3 ± 1.6	7.9 ± 1.9	198.7 ± 88.6	11

Parameters for passive membrane properties were calculated according to the model described by Llano et al. (1991), which distinguishes two regions of Purkinje cells: region 1 representing the soma and the main proximal dendrites and region 2 representing the dendritic tree. C1 and C2 represent the lumped membrane capacitance of regions 1 and 2, respectively. R1 represents the pipette access resistance. Region 2 is linked to region 1 by resistor R2, which represents the lumped resistance between the main proximal dendrite and each membrane region of the distal dendrites. R3 represents the lumped resistance of the dendritic tree of PCs.
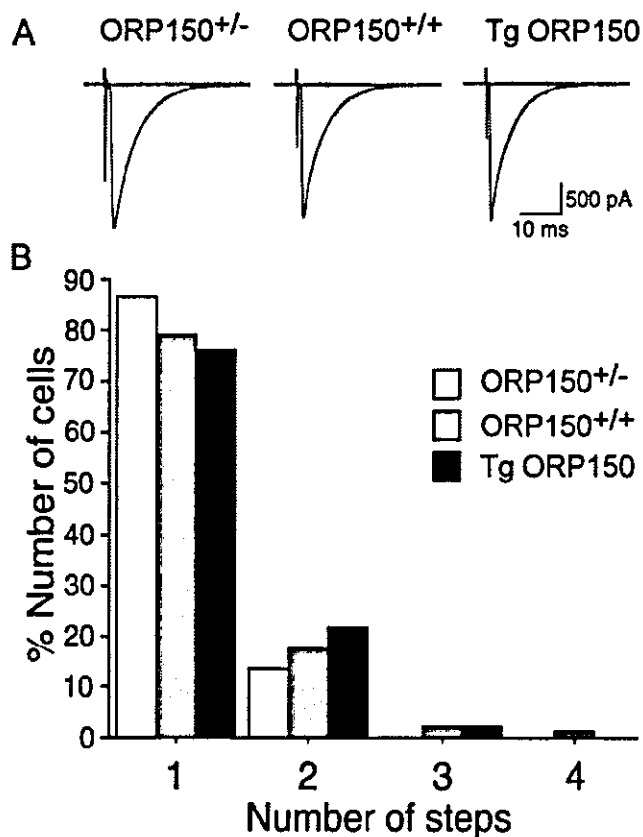
Figure 7. CF innervation of Purkinje cells in ORP150 genetically manipulated mice. A, Sample traces of CF-EPSCs recorded from ORP150 $^{+/-}$, ORP150 $^{+/-}$, and Tg ORP150 Purkinje cells. CFs were stimulated in the granular layer at 0.2 Hz, holding the potential at −20 mV. Two or three traces are superimposed at threshold stimulus intensity. B, Summary histograms showing the number of discrete steps of CF-EPSCs for ORP150 $^{+/-}$ (open columns; $n = 45$), ORP150 $^{-/+}$ (shaded columns; $n = 91$), and Tg ORP150 (filled columns; $n = 46$) Purkinje cells. There was no significant difference in the distributions for the three types of Purkinje cells ($p < 0.05$, χ^2 test for independent samples).

Consistent with this concept, mutations in the presenilin-1 gene, a cause of familial Alzheimer's disease, also renders neurons more sensitive to glutamate stress (Guo et al., 1999), probably via modification of the ER stress response (Katayama et al., 1999).

We have demonstrated that expression of ORP150 in developing brain most likely serves a cytoprotective function in Purkinje cells. Levels of ORP150 induced during brain development are carefully balanced to allow the appropriate amount of Purkinje cell death but to preserve the necessary number of these cerebellar neurons for normal function. The subtle nature of the system was revealed by overexpression of the ORP150 transgene in Purkinje cells; the number of Purkinje cells increased in Tg ORP150 animals, but cerebellar function was suboptimal. These observations with ORP150 emphasize the importance of ER stress in the Purkinje cell response to ischemia and, most likely, a range of environmental perturbations. It is intriguing to speculate that the same mechanisms that may contribute to neuronal vulnerability to ischemia and excitotoxicity (and, potentially, other stresses), such as insufficient induction of ORP150 to uniformly prevent cell death in the larger population of neurons, may be carefully programmed to prevent excess cell survival during development, at which time such additional neurons would compromise brain function.

References

Aiba A, Kano M, Chen C, Stanto ME, Fox GD, Herrup K, Zwingman TA, Tonegawa S (1994) Deficient cerebellar long-term depression and impaired motor learning in mGluR1 mutant mice. Cell 79:377–388.

Altman J, Bayer SA (1997) An overview of the postnatal development of the rat cerebellum. In: Development of the cerebellar system (Altman J, Bayer SA, eds), pp 317–324. Boca Raton, FL: CRC.

Baader SL, Sanlioglu S, Berrebi AS, Parker-Thornburg J, Oberdick J (1998) Ectopic overexpression of engrailed-2 in cerebellar Purkinje cells causes restricted cell loss and retarded external germinal layer development at lobule junctions. J Neurosci 18:1763–1773.

Bergmann M, Fox PA, Grabs D, Post A, Schilling K (1996) Expression and subcellular distribution of glutamate receptor subunits 2/3 in the developing cerebellar cortex. J Neurosci Res 43:78–86.

Brorson JR, Manzolillo PA, Gibbons SJ, Miller RJ (1995) AMPA receptor desensitization predicts the selective vulnerability of cerebellar Purkinje cells to excitotoxicity. J Neurosci 15:4515–4524.

Calabrese V, Scapagnini G, Ravagna A, Giuffrida Stella AM, Butterfield DA (2002) Molecular chaperones and their roles in neural cell differentiation. Dev Neurosci 24:1–13.

Chena Z, Ljunggrenb HG, Bogdanovica N, Nennesmoc I, Winblada B, Zhu J (2002) Excitotoxic neurodegeneration induced by intranasal administration of kainic acid in C57BL/6 mice. Brain Res 931:135–145.

Clark HB, Orr HT (2000) Spinocerebellar ataxia type 1: modeling the pathogenesis of a polyglutamine neurodegenerative disorder in transgenic mice. Neuropathol Exp Neurol 59:265–270.

Coyle JT, Puttfarchen P (1993) Oxidative stress, glutamate, and neurodegenerative disorders. Science 262:689–695.

Craven RA, Egerton M, Stirling CJ (1996) A novel Hsp70 of the yeast ER lumen is required for the efficient translocation of a number of protein precursors. EMBO J 15:2640–2650.

Crepel F, Delhaye-Bouchaud N, Dupont JL (1981) Fate of the multiple innervation of cerebellar Purkinje cells by climbing fibers in immature control, x-irradiated and hypothyroid rats. Brain Res 227:59–71.

Dove LS, Nahm SS, Murchison D, Abbott LC, Griffith WH (2000) Altered calcium homeostasis in cerebellar Purkinje cells of leaner mutant mice. J Neurophysiol 84:513–524.

Fan H, Favero M, Vogel MW (2001) Elimination of Bax expression in mice increases cerebellar Purkinje cell numbers but not the number of granule cells. J Comp Neurol 436:82–91.

Guo Q, Fu W, Sopher BL, Miller MW, Ware CB, Martin GM, Mattson MP (1999) Increased vulnerability of hippocampal neurons to excitotoxic necrosis in presenilin-1 mutant knock-in mice. Nat Med 5:101–106.

Hafidi A, Hillman DE (1997) Distribution of glutamate receptors GluR 2/3 and NR1 in the developing rat cerebellum. Neuroscience 81:427–436.

Hata R, Matsumoto M, Hatakeyama T, Ohtsuki T, Handa N, Niinobe M, Mikoshiba K, Sakaki S, Nishimura T, Yanagihara T, Kamada T (1993) Differential vulnerability in the hindbrain neurons and local cerebral blood flow during bilateral vertebral occlusion in gerbils. Neuroscience 56:423–439.

Ito M (1984) The cerebellum and neural control. New York: Raven.

Kakizawa S, Yamasaki M, Watanabe M, Kano M (2000) Critical period for activity-dependent synapse elimination in developing cerebellum. J Neurosci 20:4954–4961.

Kano M, Hashimoto K, Chen C, Abeliovich A, Aiba A, Kurihara H, Watanabe M, Inoue Y, Tonegawa S (1995) Impaired synapse elimination during cerebellar development in PKC gamma mutant mice. Cell 83:1223–1231.

Kano M, Hashimoto K, Kurihara H, Watanabe M, Inoue Y, Aiba A, Tonegawa S (1997) Persistent multiple climbing fiber innervation of cerebellar Purkinje cells in mice lacking mGluR1. Neuron 18:71–79.

Katayama T, Imaizumi K, Sato N, Miyoshi K, Kudo T, Hitomi J, Morihara T, Yoneda T, Gomi F, Mori Y, Nakano Y, Takeda J, Tsuda T, Itoyama Y, Murayama O, Takashima A, St. George-Hyslop P, Takeda M, Tohyama M (1999) Presenilin-1 mutations downregulate the signalling pathway of the unfolded-protein response. Nat Cell Biol 1:479–485.

Kitao Y, Ozawa K, Miyazaki M, Tamatani M, Kobayashi T, Yanagi H, Okabe M, Ikawa M, Yamashima T, Tohyama M, Stern D, Hori O, Ogawa S (2001) Expression of 150 kda oxygen regulated protein (orp150), a molecular chaperone in the endoplasmic reticulum, rescues hippocampal neurons from glutamate toxicity. J Clin Invest 108:1439–1450.

Konnerth A, Llano I, Armstrong CM (1990) Synaptic currents in cerebellar Purkinje cells. Proc Natl Acad Sci USA 87:2662–2665.

Kuwabara K, Matsumoto M, Ikeda J, Hori O, Ogawa S, Maeda Y, Kitagawa K, Imuta N, Kinoshita K, Stern D, Yanagi H, Kamada T (1996) Purification and characterization of a novel stress protein, the 150-kDa oxygen-regulated protein (ORP150), from cultured rat astrocytes, and its expression in ischemic mouse brain. J Biol Chem 279:5025–5032.

Lee MS, Kwon YT, Li M, Peng J, Friedlander RM, Tsai LH (2000) Neurotoxicity induces cleavage of p35 to p25 by calpain. Nature 405:360–364.

Llano I, Marty A, Armstrong CM, Konnerth A (1991) Synaptic- and agonist-induced excitatory currents of Purkinje cells in rat cerebellar slice. J Physiol (Lond) 434:183–213.

Mariani J, Changeux JP (1981a) Ontogenesis of olivocerebellar relationships. I. Studies by intracellular recordings of the multiple innervation of Purkinje cells by climbing fibers in the developing rat cerebellum. J Neurosci 1:696–702.

Mariani J, Changeux JP (1981b) Ontogenesis of olivocerebellar relationships. II. Spontaneous activity of inferior olivary neurons and climbing fiber mediated activity of cerebellar Purkinje cells in developing rats. J Neurosci 1:703–709.

Migheli A, Attanasio A, Lee WH, Bayer SA, Ghetti B (1995) Detection of apoptosis in weaver cerebellum by electron microscopic in situ end-labeling of fragmented DNA. Neurosci Lett 199:53–56.

Miranda-Contreras L, Benitez-Diaz PR, Mendoza-Briceno RV, Delgado-Saez MC, Palacios-Pru EL (1999) Levels of amino acid neurotransmitters during mouse cerebellar neurogenesis and in histotypic cerebellar cultures. Dev Neurosci 21:147–158.

Miyazaki M, Ozawa K, Hori O, Kitao Y, Matsushita K, Ogawa S, Matsuyama T (2002) Expression of ORP150 (150 kDa oxygen regulated protein) in the hippocampus suppresses delayed neuronal cell death. J Cereb Blood Flow Metab 22:979–987.

Miyazaki T, Fukaya M, Shimizu H, Watanabe M (2003) Subtype switching of vesicular glutamate transporters at parallel fiber-Purkinje cell synapses in developing mouse cerebellum. Eur J Neurosci 17:2563–2572.

Nagai N, Hosokawa M, Itohara S, Adachi E, Matsushita T, Hosokawa N, Nagata K (2000) Embryonic lethality of molecular chaperone hsp47 knockout mice is associated with defects in collagen biosynthesis. J Cell Biol 150:1499–1506.

Netzeband JG, Trotter C, Caguioa JN, Gruol DL (1999) Chronic ethanol exposure enhances AMPA-elicited Ca2+ signals in the somatic and dendritic regions of cerebellar Purkinje neurons. Neurochem Int 35:163–174.

Ogawa S, Gerlach H, Esposito C, Macaulay AP, Brett J, Stern D (1990) Hypoxia modulates the barrier and coagulant function of cultured bovine endothelium. J Clin Invest 85:1090–1098.

Ozawa K, Kuwabara K, Tamatani M, Yakatsuji K, Tsumakoto Y, Kaneda S, Yanagi H, Stern D, Ogawa S, Tohyama M (1999) ORP150 (150 kDa oxygen-regulated protein) suppresses hypoxia-induced apoptotic cell death. J Biol Chem 274:6397–6404.

Ozawa K, Tsukamoto Y, Hori O, Kitao Y, Yanagi H, Stern D, Ogawa S (2001) Regulation of tumor angiogenesis by ORP150, an inducible endoplasmic reticulum chaperone. Cancer Res 61:4206–4213.

Patil C, Walter P (2001) Intracellular signaling from the endoplasmic reticulum to the nucleus: the unfolded protein response in yeast and mammals. Curr Opin Cell Biol 13:349–355.

Sasahara M, Freis JW, Rains EW, Gown AM, Westrum LE, Frosch MP, Bonthron DT, Ross R, Collins T (1991) PDGF B-chain in neurons of the central nervous system, posterior pituitary, and in a transgenic model. Cell 64:217–227.

Selimi F, Doughty M, Delhaye-Bouchaud N, Mariani J (2000) Target-related and intrinsic neuronal death in Lurcher mutant mice are both mediated by caspaea-3 activation. J Neurosci 20:992–1000.

Shahbazian MD, Orr HT, Zoghbi HY (2001) Reduction of Purkinje cell pathology in SCA1 transgenic mice by p53 deletion. Neurobiol Dis 8:974–981.

Sieber FE, Palmon SC, Traystman RJ, Matrin LJ (1995) Global incomplete cerebral ischemia produces predominantly cortical neuronal injury. Stroke 26:2091–2096.

Siesjoe BK (1988) Mechanisms of ischemic brain damage. Crit Care Med 16:954–963.

Stacchiotti A, Schiaffonati L, Tiberio L, Rodella L, Bianchi R (1997) Constitutive expression of heat shock proteins 70 and 90 in rat cerebellum. Eur J Histochem 41:127–132.

Tamatani M, Matsuyama T, Yamaguchi A, Mitsuda N, Tsukamoto Y, Taniguchi T, Che YH, Ozawa K, Hori O, Nishimura H, Yamashita A, Okabe M, Yanagi H, Stern DM, Ogawa S, Tohyama M (2001) ORP150 protects against hypoxia/ischemia-induced neuronal death. Nat Med 7:317–323.

Urano F, Wang X, Bertolotti A, Zhang Y, Chung P, Harding HP, Ron D (2000) Coupling of stress in the ER to activation of JNK protein kinases by transmembrane protein kinase IRE1. Science 287:664–666.

Wang XZ, Lawson B, Brewer JW, Zinszner H, Sanjay A, Mi LJ, Boorstein R, Kreibich G, Hendershot LM, Ron D (1996) Signals from the stressed endoplasmic reticulum induce C/EBP-homologous protein (CHOP/GADD153). Mol Cell Biol 16:4273–4280.

Welsh JP, Yuen G, Placantonakis DG, Vu TQ, Haiss F, O'Hearn E, Molliver ME, Aicher SA (2002) Why do Purkinje cells die so easily after global brain ischemia? Aldolase C, EAAT4, and the cerebellar contribution to posthypoxic myoclonus. Adv Neurol 89:331–359.

Wynn RM, Davie JR, Cox RP, Chuang DT (1994) Molecular chaperones: heat-shock proteins, foldases, and matchmakers. J Lab Clin Med 124:31–36.

Yoshida M, Yamashima T, Zhao L, Tsuchiya K, Kohda Y, Tonchev AB, Matsuda M, Kominami E (2002) Primate neurons show different vulnerability to transient ischemia and response to cathepsin inhibition. Acta Neuropathol (Berl) 104:267–272.

Yu Z, Luo H, Fu W, Mattson MP (1999) The endoplasmic reticulum stress-responsive protein GRP78 protects neurons against excitotoxicity and apoptosis: suppression of oxidative stress and stabilization of calcium homeostasis. Exp Neurol 155:302–314.

Zanjani HS, Vogel MW, Delhaye-Bouchaud N, Martinou JC, Mariani J (1996) Increased cerebellar Purkinje cell numbers in mice overexpressing a human bcl-2 transgene. J Comp Neurol 374:332–341.

Zhao HM, Wenthold RJ, Petralia RS (1998) Glutamate receptor targeting to synaptic populations on Purkinje cells is developmentally regulated. J Neurosci 18:5517–5528.

ORP150/HSP12A protects renal tubular epithelium from ischemia-induced cell death

YOSHIO BANDO,*[,1,2] YOSHITANE TSUKAMOTO,[†,1] TAICHI KATAYAMA,[‡]
KENTARO OZAWA,[§] YASUKO KITAO,[§] OSAMU HORI,[§] DAVID M. STERN,[1]
ATSUSHI YAMAUCHI,[||] AND SATOSHI OGAWA[§]

*Department of Anatomy I, Asahikawa Medical College, Asahikawa, Hokkaido, Japan; [†]Department of Pathology, Osaka Medical Center for Cancer and Cardiovascular Diseases, Higashinari, Osaka, Japan; [‡]Department of Anatomy and Neuroscience, Osaka University Medical School, Yamada Oka, Japan; Division of Nephrology, Department of Medicine, Osaka Rosai Hospital, Sakai, Japan; [§]Department of Neuroscience, Kanazawa University Medical School, Kanazawa City, Ishikawa, Japan; and [1]Dean's Office, Medical College of Georgia, Augusta, Georgia, USA

SPECIFIC AIMS

Renal cell injury caused by ischemia/reperfusion (I/R) is often accompanied by acute failure of renal function, which is clinically of importance due to high mortality. 150 kDa oxygen-regulated protein (ORP150) is an inducible endoplasmic reticulum (ER) chaperone with cytoprotective properties in settings of cell stress, such as ischemia/reperfusion (I/R). Based upon the cytoprotective properties of 150 kDa oxygen regulated protein (ORP150) in ischemic condition, we have examined the role of ORP150 in renal ischemia/reperfusion (I/R).

PRINCIPAL FINDINGS

1. ORP150 is expressed in renal epithelial cells in both human and rat kidney after I/R

In acute tubular necrosis accompanying cardiogenic shock, ORP150 was detected mainly in parts of renal tubules in the cortex, and, more frequently, in the medulla. The same pattern of ORP150 expression was found in a case of osmotic nephrosis due to treatment of brain edema.

To further analyze expression of ORP150, rats were subjected to renal I/R by unilateral occlusion of the renal artery. Northern blot showed a marked increase in ORP150 transcripts after I/R on the ipsilateral side, peaking 8–12 h after reperfusion (**Fig.** 1A). ORP150 transcripts were also induced on the contralateral side, though to a lesser extent (Fig. 1B). In situ hybridization of normal kidney revealed a diffuse distribution of ORP150 transcripts in the medulla (Fig. 1C, G). ORP150 transcripts were strongly induced 12 h after I/R in the outer medulla, the area between cortex and medulla (Fig. 1D, E, H, I). Distribution of ORP150 transcripts overlapped, at least partially, with that ob-

served for Tamm-Horsefall protein (THP) mRNA (Fig. 1F), a marker of the thick ascending loop (TAL). Immunohistochemical analysis of normal rat kidney displayed low-level expression of ORP150 antigen in the renal medulla (Fig. 1J), whereas no signal was detected in the cortex (Fig. 1K). After I/R, ORP150 antigen was markedly induced in renal tubules within the medulla (Fig. 1L), as well as in portions of renal tubules in the cortex (Fig. 1M).

2. ORP150 suppresses cell death in renal epithelial cells

Exposure of MDCK cells, a renal tubular epithelial cell line, to hypoxia caused expression of ORP150 antigen; the latter increased by 12 h and reached a maximum between 24–48 h. Incubation of MDCK cultures in presence of high salt (NaCl, 300 mM) also induced ORP150 antigen. Combination of hypoxia and hyperosmolarity appeared to potentiate ORP150 expression to levels greater than that observed with either stimulus alone. Stable transfectants of MDCK cells were made with antisense or sense constructs of human ORP150. After exposure of these stably transfected cell lines to hypoxia (24 h), antisense transfectants demonstrated detectable, but low levels of ORP150 antigen; vector-alone transfectants showed higher levels of ORP150; and sense transfectants displayed highest levels of ORP150. To evaluate vulnerability of MDCK stable transfectants to hypoxia and hyperosmolar stress, cultures were exposed to hypoxia in presence of NaCl (500 mM) for 36 h, and cell death was evaluated by release of

---

[1] These authors contributed equally to this work.

[2] Correspondence: Department of Anatomy I, Asahikawa Medical College, Midorigaoka-Higashi 2-1-1-1, Asahikawa, 078-8510, Hokkaido, Japan. E-mail: ybando@asahikawa-med.ac.jp
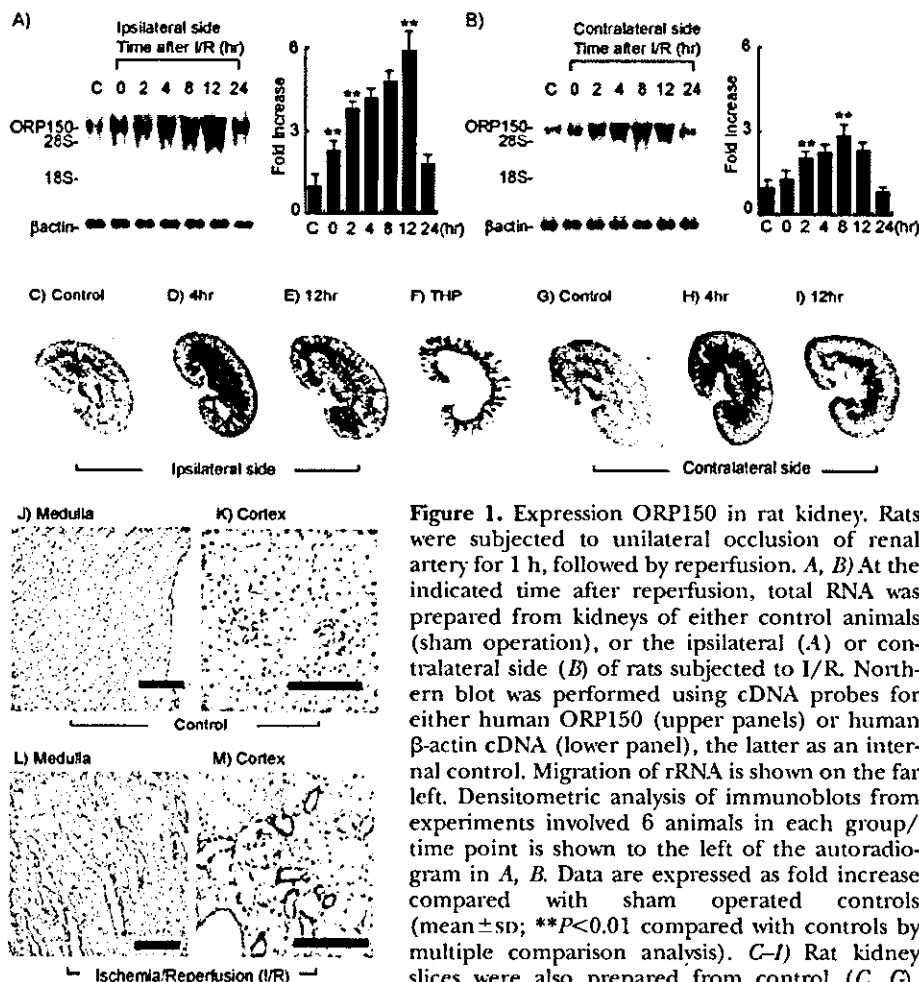
Figure 1. Expression ORP150 in rat kidney. Rats were subjected to unilateral occlusion of renal artery for 1 h, followed by reperfusion. *A, B)* At the indicated time after reperfusion, total RNA was prepared from kidneys of either control animals (sham operation), or the ipsilateral (*A*) or contralateral side (*B*) of rats subjected to I/R. Northern blot was performed using cDNA probes for either human ORP150 (upper panels) or human β-actin cDNA (lower panel), the latter as an internal control. Migration of rRNA is shown on the far left. Densitometric analysis of immunoblots from experiments involved 6 animals in each group/ time point is shown to the left of the autoradiogram in *A, B.* Data are expressed as fold increase compared with sham operated controls (mean±SD; **$P<0.01$ compared with controls by multiple comparison analysis). *C–I)* Rat kidney slices were also prepared from control (*C, G*), ipsilateral (*D, E*), and contralateral side (*H, I*) 4 and 12 h after reperfusion, and subjected to in situ hybridization using human ORP150 probe. *F)* Images obtained with kidney slices from control mice analyzed by in situ hybridization using human Tamm-Horsefall protein (THP). Adjacent sections of control (*J, K*) and ipsilateral I/R kidney (*L, M*; 12 h after reperfusion) were subjected to immunohistochemical analysis using β-human ORP150 antibody. Filled bars in each panel represent 100 μm.

LDH and induction of apoptosis by activation of caspase-3. Results demonstrate increased cell death and activated caspase-3 in antisense transfectants and lowest levels of cell death/activated caspase-3 in sense transfectants. These data indicate a correlation between expression of ORP150 and cellular resistance to hypoxia/hyperosmolar-induced cell death.

3. Furosemide suppressed expression of ORP150 transcripts by unilateral nephrectomy and I/R

The effect of furosemide (a loop diuretic) on ORP150 expression after unilateral nephrectomy and I/R was assessed. Unilateral nephrectomy induced ORP transcripts in the remaining kidney, with peak expression 8–12 h after the procedure. Unilateral I/R also caused prominent up-regulation of ORP150 mRNA, in this case in both kidneys with the most striking effect on the ipsilateral side. Pretreatment with furosemide sup-
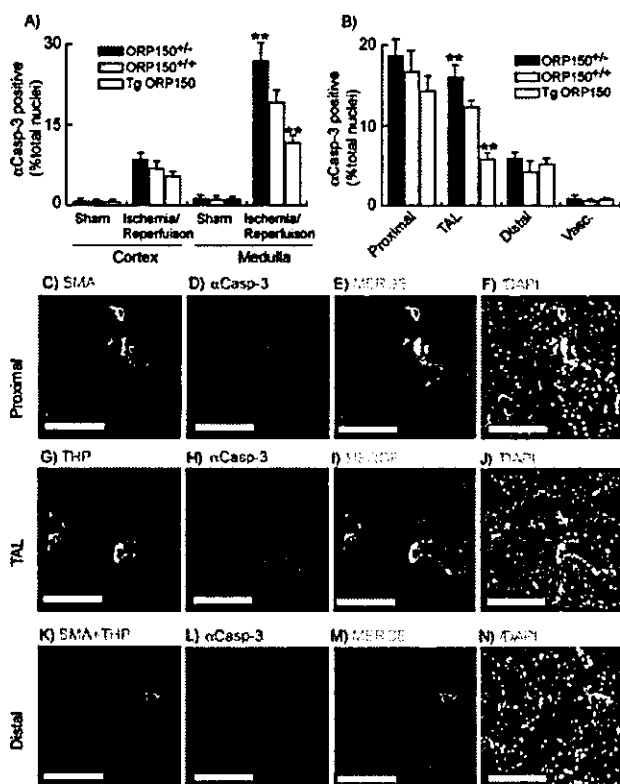
pressed expression of ORP150 mRNA in both unilateral nephrectomy and I/R. This suggests the possibility that increased ORP150 mRNA observed in both contralateral/ipsilateral kidneys after I/R may be due to osmotic stress, at least in part.

4. ORP150 suppressed renal dysfunction in a murine model after I/R, by protecting cell viability in TAL
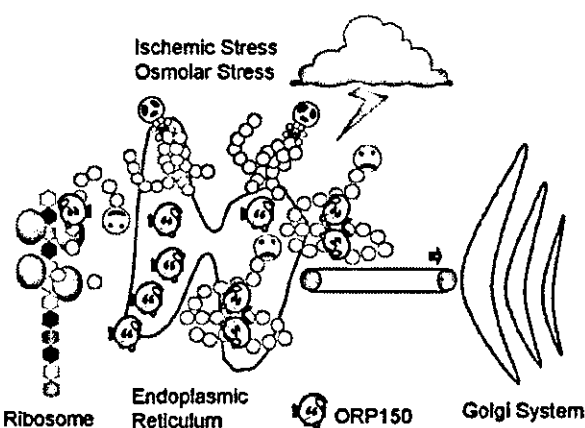
Mice with genetically manipulated expression of ORP150 were used to assess the effect of ORP150 on renal function following I/R injury. For these studies, mice were prepared by right nephrectomy followed seven days later by occlusion of the left renal pedicle for 45 min (I or ischemia) and reperfusion (R). Tg ORP150 mice displayed relative resistance to renal dysfunction, based on the blunted rise in serum creatinine and serum/blood urea nitrogen compared with ORP150$^{+/-}$ animals. Caspase-3 activity was assessed in

renal tissue as an index of programmed cell death. Highest levels were observed in ORP150$^{+/-}$ animals, intermediate levels in ORP150$^{-/+}$ mice, and lowest levels in Tg ORP150 mice.

To further localize the protective effect of ORP150 expression on the kidney, immunohistochemical studies were performed with an antibody selective for activated caspase-3 and renal tubular markers. In the renal cortex, there was no significant difference in the proportion of nuclei staining positively with caspase-3

Figure 3. Hypoxia and osmolar stress are directed to a cellular organelle, ER.

antibody comparing mice of each genotype (Fig. 2A). In medulla, caspase-3-positive nuclei were most frequently observed in ORP150$^{+/-}$ mice, whereas they were least abundant in Tg ORP150 animals (Fig. 2A). Since caspase-3-positive signals identified by this method were likely to include deteriorating cells in casts, we further sought to map distribution of potentially apoptotic cells in portions of the renal segment (Fig. 2B–N). Although there was no significant difference in the percentage of caspase-3-positive nuclei in proximal and distal renal tubules between the three genotypes, there were differences in TAL based on colocalization with THP (Fig. 2B). These data suggest that overexpression of ORP150 in the kidney enhances cellular viability in response to ischemic challenge, especially in TAL.

CONCLUSIONS AND SIGNIFICANCE

We have identified ORP150 as a stress protein expressed in I/R-mediated injury to the kidney. ORP150 appears to have a cytoprotective effect on renal epithelial cells both in vitro and in vivo in response to I/R and hyperosmolar stress. Though the precise mechanism through which ORP150 exerts its cytoprotective effect in TAL remains to be defined, it is likely to involve its chaperone-like properties in the ER. Since cytoprotective effects of ORP150 (an ER chaperon) were focused on TAL, we suggest that maintenance of ER function is an essential component of a successful stress response in this portion of the nephron in acute renal failure.

Data presented in this manuscript indicate that ORP150 is also induced in response to hyperosmolar stress, and this is accentuated by superimposed oxygen deprivation. Our data suggest that both ischemic and osmolar stress targets a cellular organelle (ER) resulting in an accumulation of immature and unfolded proteins inside (Fig. 3). Resistance of MDCK cells to this complex environmental challenge is dependent at least in part on ORP150.

Figure 2. Effect of ORP150 on viability of renal tubular segments. A) 1 wk after unilateral nephrectomy, ORP150$^{+/-}$ (filled bars), ORP150$^{+/+}$ (shaded bars), or Tg ORP150 (open bars) mice were subjected to I/R (of remaining kidney) or sham procedure (i.e., the latter animals only received nephrectomy). 24 h after I/R, mice were killed and renal sections were incubated with α-activated caspase-3 antibody, followed by staining with DAPI. Nuclei staining positive for activated caspase-3 were counted in the cortex and medulla, and values were expressed as % positive nuclei (total nuclei were determined by DAPI staining). Mean ± SD is shown (n=6); **P < 0.05 vs. observations in ORP150$^{-/+}$ mice, by multiple comparison analysis. B) Sections were double-stained with segment markers and α-activated caspase-3 antibody. In each segment, nuclei staining positive with α-activated caspase-3 antibody were counted and values were expressed as % total nuclei (the latter determined by DAPI staining). The same procedure was also performed in a renal arteriole (Vasc.). Mean ± SD is shown (n=6). C–N) Representative images obtained in ORP150$^{+/-}$ mice are shown. Immunofluorescent images obtained with markers of tubular segments (green; C, G, K) and α-activated caspase-3 antibody (red; D, H, L) were digitally overlapped (E, I, M). Latter images were further merged with results of nuclear staining using DAPI (light blue; F, J, N). In each panel, open bars represent 100 μm.

Review

Ca^{2+}-dependent proteases in ischemic neuronal death A conserved 'calpain–cathepsin cascade' from nematodes to primates

Tetsumori Yamashima*

Department of Neurosurgery, Division of Neuroscience, Kanazawa University Graduate School of Medical Science, Takara-machi 13-1, Kanazawa 920-8641, Japan

Received 8 February 2004

Abstract

From rodents to primates, transient global brain ischemia is a well known cause of delayed neuronal death of the vulnerable neurons including cornu *Ammonis* 1 (CA1) pyramidal cells of the hippocampus. Previous reports using the rodent experimental paradigm indicated that apoptosis is a main contributor to such ischemic neuronal death. In primates, however, the detailed molecular mechanism of ischemic neuronal death still remains obscure. Recent data suggest that necrosis rather than apoptosis appear to be the crucial component of the damage to the nervous system during human ischemic injuries and neurodegenerative diseases. Currently, necrotic neuronal death mediated by Ca^{2+}-dependent cysteine proteases, is becoming accepted to underlie the pathology of neurodegenerative conditions from the nematode *Caenorhabditis elegans* to primates. This paper reviews the role of cysteine proteases such as caspase, calpain and cathepsin in order to clarify the mechanism of ischemic neuronal death being triggered by the unspecific digestion of lysosomal proteases.
© 2004 Elsevier Ltd. All rights reserved.

Keywords: Hippocampus; Ischemic neuronal death; Caspase; Calpain; Cathepsin; Calpain–cathepsin hypothesis

1. Introduction

The human brain is a sophisticated and complex organ in which about 100 billion neurons are assembled in circuits working together. When a nerve impulse arrives in the presynaptic axon terminal, neurotransmitters are released from the synaptic vesicles into the synaptic cleft. Neurotransmitters then bind to specific receptors in the postsynaptic neuron, causing influx of extracellular Na$^+$ through membrane ion channels. The action potential (nerve impulse) is simply a brief reversal of the resting potential; the inside of the membrane becomes positively charged with respect to the outside within a thousandth of second.

The Ca^{2+} concentration is approximately 1–2 mM at the synaptic cleft whereas and ~100 nM in the cytosol, thereby generating a 10,000–20,000-fold gradient between outside and inside of the synapse. In the hippocampal neurons, for instance, the presynaptic activation causes a release of glutamate into the synaptic cleft, which acts on the postsynaptic AMPA or NMDA receptors. At resting potential, Na$^+$ passes through AMPA receptor while NMDA receptor is blocked with Mg^{2+} without Ca^{2+} influx. At depolarized potentials the block is removed and Ca^{2+} enters the postsynaptic neurone.

Under physiological conditions, the intracellular Ca^{2+} concentration is tightly regulated. In contrast, under pathological conditions, regulatory mechanisms are overwhelmed and the intracellular Ca^{2+} concentration increases abnormally via two main routes: influx from extracellular pools through various channels and release from endoplasmic reticulum stores. Disruption of intracellular Ca^{2+} homeostasis has been implicated in various forms of neuronal death and neurodegeneration from nematodes to mammals [1–4].

Various proteins in the neuronal membrane including receptors and channels, give rise to the unique capabilities of neurons to transmit, receive and store information. The rough ER synthesizes such membrane proteins, neurotransmitters, cytoskeleton proteins and other constituent proteins. For the post-translational processing, degradation, recycling

*Tel.: +81-76-265-2381; fax: +81-76-234-4262.
E-mail address: yamashim@med.kanazawa-u.ac.jp (T. Yamashima).

61 or turnover of the abundant proteins, lysosomal hydrolytic
62 proteases are indispensable.
63   The lysosomal membrane is a physical barrier that pre-
64 vents hydrolytic enzymes from digesting the cell's own cy-
65 toplasm, but its severe damage can cause cell necrosis. In
66 1966, de Duve and Wattiaux [5] reported that the lethal cell
67 injury occurs by the release of hydrolytic enzymes from the
68 damaged lysosomes. In the execution of neuronal necrosis,
69 the mechanisms of abnormal protein degradation mediated
70 by lysosomal proteases could conceivably play an impor-
71 tant role. Cysteine proteases, a set of lysosomal enzymes,
72 represent a broad class of proteolytic enzymes widely dis-
73 tributed among living organisms. Cysteine proteases are ac-
74 tually recognized as multi-function enzymes, being involved
75 in the processing and presentation of antigens, cleavage of
76 membrane-bound proteins, degradation of the cellular ma-
77 trix, and in the processes of tissue remodeling. Here, the
78 role of Ca^{2+}-dependent cysteine proteases in the execution
79 of neuronal necrosis will be reviewed.

80 2. Different mode of neuronal death

81   Necrosis and apoptosis are two distinct forms of cell
82 death which have, essentially, different implications for the
83 surrounding tissue. Necrosis occurs ATP-independently in
84 the process of neurodegeneration, provoking damage to
85 the tissue with spillage of the intracellular contents into
86 the extracellular milieu. In contrast, apoptosis occurs ATP-
87 dependently, without provoking inflammation and damage
88 to the tissue. Further, apoptosis is programmed and essential
89 for the normal development, shaping of organs and tissues,
90 and homeostatic mechanisms [6–8]. In contrast, necrosis is
91 unanticipated and inappropriate destruction of a cell, that is
92 caused by certain stressful or abnormal conditions exceed-
93 ing a certain threshold such as stroke, excessive mechanical
94 strain (trauma) and genetic abnormalities underlying neu-
95 rodegenerative diseases [9–13].
96   During development of the brain, neuronal death oc-
97 curs mainly by caspase-dependent apoptosis [2,14] or au-
98 tophagy, morphologically and mechanistically distinct [15].
99 In the adult brain, however, caspase-dependent apoptosis
100 should be essentially minor [2]. In the animal models of
101 neurodegeneration, the dominant forms of neuronal death
102 are dark neuronal death in Huntington's disease [16] or
103 paraptosis in amyotrophic lateral sclerosis [17]. Paraptosis
104 is characterized by the extensive cytoplasmic vacuolation
105 without prominent chromatin condensation. In this process,
106 the morphology is similar to necrosis while the cascade of
107 de novo protein synthesis is similar to apoptosis. Excito-
108 toxic neuronal death due to cerebral ischemia or traumatic
109 brain injury, may show many shapes and activate different
110 cell death programmes. Necrotic rather than apoptotic cas-
111 cade [18,19] or mixed apoptotic–necrotic cascades may be
112 involved, depending on the intensity of insult, the age of
113 subjects, and the brain region affected [20,21]. For instance,

114 in the ischemic core, caspases are inactivated because of
115 the rapid ATP depletion, impairment of the intracellular
116 ion composition, massive production of nitric oxide or
117 superoxide radicals as well as calpain activation [22–28].
118 The sustained calpain activation in the postischemic CA1
119 neurons caused long-standing lysosomal membrane dis-
120 ruption with the resultant leakage of various hydrolytic
121 enzymes including cathepsins B, L and DNase II, processes
122 that start immediately after ischemia and last until day 5
123 [19].
124   Although there are many reports of apoptotic death of
125 neurons in the ischemic stroke models using adult animals,
126 relatively few of them have been based on detection of the
127 characteristic morphological features of apoptosis. Histo-
128 logical examination of hippocampus in a 63-year-old fe-
129 male dying 9 days after heart surgery undergoing transient
130 cardiac arrest, showed an almost complete neuronal death
131 specifically in the CA1 sector [28]. Here, all of the dy-
132 ing CA1 neurons showed a typical eosinophilic degenera-
133 tion which was characterized by the shrunken eosinophilic
134 cytoplasm and the nucleus with a coarse tigroid and thin
135 chromatin distribution. However, there was no morphologi-
136 cal evidence of apoptosis. In the postischemic CA1 neuronal
137 death of monkeys [18,29–31], light microscopy showed sim-
138 ilar eosinophilic coagulation necrosis, while electron mi-
139 croscopy showed frank membrane disruptions with punctu-
140 ated chromatin condensation. Furthermore, DNA gel elec-
141 trophoresis showed not ladder but smear pattern [18,19]. Ac-
142 cordingly, it is likely that even if the apoptosis cascade was
143 actually activated, the final neuronal death pattern was that
144 of necrosis.
145   Despite the significant impact of necrotic neuronal death
146 in human brain injury and neurodegenerative diseases, the
147 mechanism of neuronal necrosis remained poorly under-
148 stood until recently. As models of neuronal necrosis and
149 neurodegeneration became available, from *C. elegans* [32]
150 to monkeys [28,29,33], a common denominator becomes in-
151 creasingly clear. In contrast to the events taking place during
152 apoptosis, in necrosis it is not the mobilization of molecular
153 mechanisms but the excessive operation of the physiological
154 cellular mechanisms that appear to execute neuronal necro-
155 sis process under the exceptional cell conditions that lead to
156 extensive damage.

3. Three cysteine proteases   157

3.1. Caspase   158

159   In animal models of neuronal death, apoptosis of neurons
160 has been often demonstrated only by terminal deoxynu-
161 cleotidyl transferase-mediated deoxyuridine triphosphate
162 (dUTP) nick end-labelling (TUNEL) without detecting
163 the characteristic morphological features of apoptosis.
164 Accordingly, there are many reports that conclude that
165 neuronal apoptosis after ischemia is mediated by cysteine-

requiring aspartate-directed proteases, caspases. However, the TUNEL technique was reported to label also cells undergoing necrosis [34–36]. Thus, even if caspases are activated, it is probable that they contribute more to neuronal necrosis than to neuronal apoptosis.

Caspases are mammalian homologues of the pro-apoptotic *C. elegans* CED-3 protein. In their catalytic site caspases contain the cysteine-containing pentapeptide motif QACXG (X being R, Q or G) and require an aspartate residue at the N-terminal end of the substrate cleavage site [37–41]. Caspases are synthesized as inactive proenzymes (procaspases) that comprise an N-terminal prodomain, a large subunit, and a small subunit. Activation results from the proteolytic cleavage of procaspases into its three component parts through the action of other activated caspases. Subsequently, two large and two small subunits associate to form the heterotetrameric active enzyme. The substrates cleaved by caspases include cytoskeletal and associated proteins, kinases, members of the Bcl-2 family of apoptosis-related proteins, presenilins and amyloid precursor protein, and DNA-modulating enzymes. Many of the substrates of caspases are localized in the pre- and/or post-synaptic compartments of neurons.

Caspases are believed to be central components for the implementation of neuronal apoptosis [42]. Caspase-3 was demonstrated to be overexpressed in CA1 after transient ischemia, and its specific inhibitor could attenuate ischemic neuronal death [43,44]. In the monkey experimental paradigm of cerebral ischemia also [18,19], caspase-3 activation occurred a few hours after ischemia, but its activation became negligible despite up-regulation of pro-caspase-3 on days 3–5. The caspase-activated DNase (CAD)/inhibitor of CAD (ICAD) complex was identified to be a substrate of caspase-3 [45–47]. When the catalytically-active caspase-3 cleaves ICAD, the final effector CAD transfers into the nucleus to cause DNA degradation [46–48]. Cao et al. [49] reported that transient global ischaemia in rats caused caspase-3-mediated cleavage of ICAD, resulting in the apoptotic degradation of DNA by CAD. Although expression of CAD was slightly up-regulated on days 1 and/or 2 with translocation of activated CAD on days 2–3 in the monkey experimental paradigm [18,19], the extent of CAD expression was actually much less compared to lymph node or intestine tissues. It is likely that CAD has partially participated in DNA degradation of the postischemic CA1 neurons in monkeys. However, as CAD up-regulation was mild and occurred transiently on days 1–2 in monkeys, calpain activation lasting as long as 5 days appears to be a rather critical factor for the CA1 neuronal death being completed on days 3–5 [19].

3.2. Calpain

The calcium-dependent neutral cysteine protease, calpain, is present in virtually all vertebrate cells [50,51].

Two isozymes: μ- and m-calpains show similar biochemical features, except for the Ca^{2+} concentration necessary for activation in vitro: μ- or m-calpains require micromolar or milimolar levels of Ca^{2+}, respectively. Calpain is a heterodimer comprising a 30-kDa regulatory subunit and another 80-kDa catalytic subunit. During activation, the 30-kDa subunit is cleaved to yield a final 17-kDa form, while the 80-kDa subunit is converted to 76-kDa enzymatically active form. Calpain is activated both in physiological states and also during various pathological conditions such as phosphorylation [52], free radicals [53,54], brain ischemia-reperfusion [19,29], apoptosis [53,55], cataractogenesis [56], muscular dystrophy [57], and Alzheimer's [58] and Parkinson's [59] diseases. The substrates cleaved by μ-calpain include cytoskeletal and associated proteins, kinases and phosphatases, membrane receptors and transporters, and steroid receptors. Calpains are located throughout the neuron, both in the somatodendritic regions and in the axons. Excessive activation of calpain due to an increase in free Ca^{2+} leads to cytoskeletal protein breakdown, subsequent loss of structural integrity and disturbances of axonal transport, and finally to neuronal death.

What is the in vivo substrate of activated μ-calpain in the postischemic CA1 neurons? As calpain cleaves the substrate protein without binding, one cannot detect the in vivo substrate of activated calpain, for example, by means of immunoprecipitation. Further, regarding the cleavage site specificity of calpain, there are suggestions that the PEST sequence is preferred, as generally indicated, but this issue is not firmly confirmed. It was recently speculated that calpain recognizes the conformational state rather than the protein sequence; relatively unstructured inter-domain sequences without α-helix or β-sheet seem to be good targets [60]. Therefore, as for most proteases, it is either impossible or not relevant to predict a calpain cleavage site in a given protein only based on the sequence information. Accordingly, instead of the use of biochemical procedures, we have demonstrated, by means of immunoelectron microscopy, the localization of activated μ-calpain at the lysosomal membrane [28,29]. Recently, we also reported sustained (i.e., from immediately after the ischemic challenge until day 5) activation of μ-calpain in the postischemic CA1 neurons [19]: the immunoreactivity of activated μ-calpain became maximal on days 2–3, being remarkable in lysosomes on day 2 while in the cytoplasm on day 3 (Fig. 1). The subsequent translocation of lysosomal cathepsins [28,33] as well as lysosome-associated membrane protein-1 (LAMP-1) (Fig. 2) indicated that activated μ-calpain caused spillage of hydrolytic enzyme cathepsins from lysosomes [19].

In neurological events associated with cerebral ischemia, Alzheimer's disease, Parkinson's disease and amyotrophic lateral sclerosis, a potential role of reactive oxygen species has been reported [61,62]. Another possible mechanism of lysosomal membrane rupture might be the damage induced
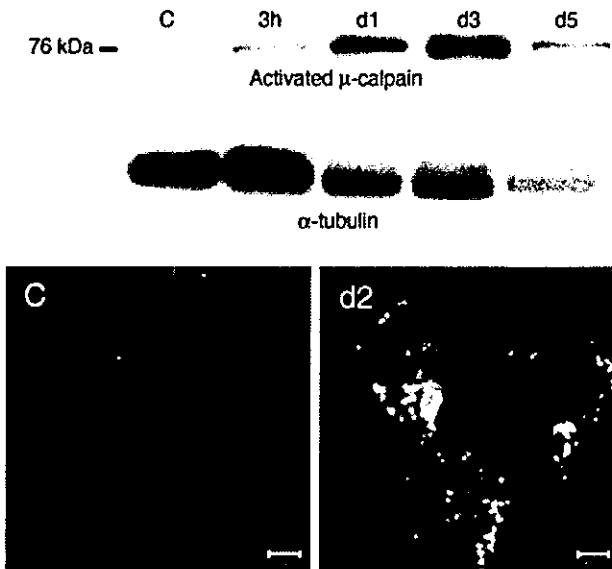
Fig. 1. Immunoblot analysis (upper) and immunofluorescent confocal images (lower), using antibody recognizing selectively activated μ-calpain. Upper: The expression of the internal control protein α-tubulin shows a gradual decrease on days 1–5 (d1, d3, d5) with neuronal degeneration. In contrast, activated μ-calpain is up-regulated from 3 h after ischemia until day 5 (d5), and is maximal on day 3 (d3) in the postischemic CA1 sectors. Lower: In the control CA1 neurons (C), the perikarya shows negligible immunostaining of activated μ-calpain. In contrast, on day 2 (d2) activated μ-calpain is immunostained as coarse granules with FITC in the perikarya. Scale bar = 5 μm.

276 by free radicals that are generated during the oxidative stress.
277 Then, as a consequence of exposure to reactive oxygen
278 species, oxidative stress may induce further calpain activa-
279 tion through rapid Ca^{2+} mobilization either by stimulating
280 Ca^{2+} influx from outside or by increasing Ca^{2+} release from
281 the internal stores [63,64].

282 3.3. Cathepsin

283 Brunk et al. [65] suggested a quantitative relationship
284 between the amount of lysosomal rupture and the mode of
285 cell death: low intensity stresses would trigger a limited
286 release of lysosomal enzymes to the cytoplasm followed
287 by apoptosis, whereas high intensity stresses would pro-
288 voke a generalized lysosomal rupture followed by necrosis.
289 The lysosomal membrane is a physical barrier prevent-
290 ing hydrolytic enzymes from digesting the cell constituent
291 proteins, but its severe disruption can cause cell necrosis
292 in the pathologic states. The spreading of hydrolytic en-
293 zymes into the cytoplasm through the lysosomal membrane
294 injury or rupture, was confirmed in both heart [66–68]
295 and brain [25,33,69] ischemic injuries. It is most likely
296 that the sustained calpain activation in the postischemic
297 CA1 neurons, presumably with the aid of reactive oxygen
298 species, may cause lysosomal membrane disruption with
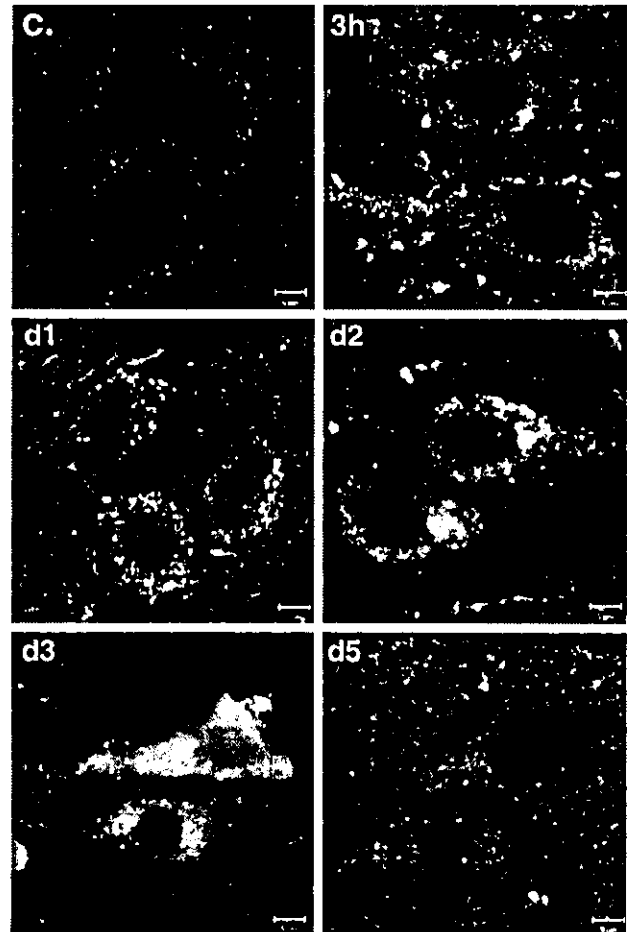299 the resultant leakage of various hydrolytic enzymes (Fig. 3)
300 [19,28].

Fig. 2. Immunofluorescent confocal images of the lysosome-associated membrane protein (LAMP)-1 in the representative CA1 neurons of the control (C), immediate after ischemia (3 h), days 1 (d1), 2 (d2), 3 (d3) and 5 (d5). The LAMP-1 immunoreactivity is up-regulated in the perikarya from 3 h until day 5 (d5). Coarse granular staining becomes maximal on day 2 (d2), while the perikarya and the nucleus are diffusely stained on day 3 (d3). On day 5 (d5), the immunoreactivity decreases with neuronal degeneration. Scale bar = 5 μm

301 Lysosomes contain over 80 types of hydrolytic enzymes.
302 Two classes of lysosomal hydrolytic enzymes appear to be
303 most active in executing neuronal death: aspartyl (cathep-
304 sin D) and cysteine (cathepsins B, H, L) proteases. The for-
305 mer are characterized by the presence of a catalytic aspar-
306 tic amino acid residue at their active site, while the latter
307 are characterized by a catalytic cysteine residue at their ac-
308 tive site. Cathepsin D mediates execution of neuronal death
309 induced by ageing, transient forebrain ischemia and excito-
310 toxicity [70] while cathepsins B and L execute hippocampal
311 neuronal death after global ischemia [28].

312 A new L-trans-epoxysuccinyl peptide, CA-074 (N-(L-3-
313 trans-carboxyoxirane-2-cabonyl)-L-isoleucyl-L-proline) was
314 shown to inhibit cathepsin B 10,000–30,000-fold stronger
315 than cathepsins H or L [71,72]. E-64c (N-(L-3-trans-
316 carboxyoxirane-2-carbonyl)-L-leucine-3-methylbutylamide),

Fig. 3. Electronmicrograph of a CA1 neuron 2 days after 20 min whole brain complete ischemia. In the cytoplasm close to the nuclear membrane, there are numerous electron-dense granules (arrows) that were released from the lysosomes. Among the punctuated chromatin condensation are similar electron-dense granules. Scale bar = 1 µm.

the terminal agmatine of E-64 being replaced by isoalry-lamide, shows strong inhibitory activity in vivo. E-64c has been demonstrated to inhibit cathepsins H and L as well as cathepsin B [73,74]. Concerning the kinetics [71–75] of each inhibitors, the K_i of CA-074 for cathepsin B, as estimated by Dixon plots, was 2.0×10^{-9} M, whereas the K_i for cathepsins H and L was 75,000 and $233,000 \times 10^{-9}$ M, respectively. In contrast, the K_i of E-64c for cathepsins B, H and L was, as estimated by Dixon plots, 8.7, 111 and 3.5×10^{-9} M, respectively. The inhibitory effect of delayed neuronal death by E-64c was overall more remarkable than that of CA-074. This is probably because E-64c can inhibit not only cathepsins B and L but also calpains.

4. The calpain–cathepsin hypothesis

The neuroprotective effects of certain caspase inhibitors conceivably depend on mechanisms other than the inhibition of caspases, because the tetrapeptide inhibitor tyrosine–valine–alanine–aspartate–chloromethyl ketone (Ac-YVAD-cmk) was reported to rescue cultured neurons from cell death due to oxygen/glucose deprivation, by targeting lysosomal enzyme 'cathepsin B' [76]. Accordingly, to clarify the exact molecular mechanism of ischemic neuronal death, the contribution of cathepsin-mediated necrotic cascade should be studied in detail with particular attentions to the role of lysosomes.

'Calpain–cathepsin hypothesis' [33] was formulated on the basis of the experimental paradigm of global brain ischemia in the monkeys, and encompases two major players, calpain and cathepsin, as the key mediators (Fig. 4). First, an increase in the intracellular Ca^{2+} mobilization occurs in response to the ischemic insult. Second, µ-calpain is activated as long as Ca^{2+} concentration is elevated. Third, as activated µ-calpain compromises the integrity of lysosomal membranes, cathepsin proteases are liberated into the cytoplasm to induce breakdown of the cell constituent proteins. This process is reminiscent of autophagy, and supports de Duve's concept [77] of lysosomes as the cell's 'suicide bag'. Kitao et al. [78] confirmed the involvement of a similar cascade in the cultured hippocampal neurones, in which both kainate and glutamate induced the activation of µ-calpain and cathepsin B.

In addition to the ischemic injuries in the heart [66–68] and brain [25,69], the translocation of cathepsin B from lysosomes into the cytosol and nucleus was reported also for the bile salt-induced and TNF-triggered hepatic apoptosis. Similarly, Foghsgaard et al. [81] found that cathepsin B, which disappeared from the perinuclear granules (colocalizing with lysosomal markers) and distributed diffusely throughout the cell, is capable of acting as a dominant execution protease in tumor cell apoptosis induced by tumor necrosis factor. Using the monkey experimental paradigm, translocations of cathepsins B and L [28,33] as well as DNase II [18], were already suggested by immunohistochemistry in the postischemic CA1 neurons. It is suggested from these data that the sustained calpain activation in the postischemic CA1 neurons may cause long-standing lysosomal membrane disruption with the resultant consecutive leakage of lysosomal enzymes including cathepsins B, L and DNase II from immediately after ischemia until day 5. Based on the calpain–cathepsin hypothesis, Yoshida et al. [31] demonstrated in the monkey brain other than CA1 that 89.8% of caudate nucleus neurons were free from postischemic neuronal death on day 5 with 4 mg/kg of CA-074 treatment, while 75.0% of the cortical V layer neurons and 91.6% of the cerebellar neurons survived with 4 mg/kg of E-64c treatment.

Recently, Syntichaki et al. [32] reported that neuronal degeneration induced by various genetic lesions in C. elegans required the activity of the calcium-regulated CLP-1 and TRA-3 proteases (similar to calpains) as well as aspartyl proteases ASP-3 and ASP-4 (similar to cathepsins). The genes for calpain and lysosomal proteases have been detected in genetic screens for suppressors of neurodegeneration in C. elegans. This is encouraging, considering that the sophisticated genetics and molecular biology of the C. elegans neurodegeneration models have confirmed the ba-
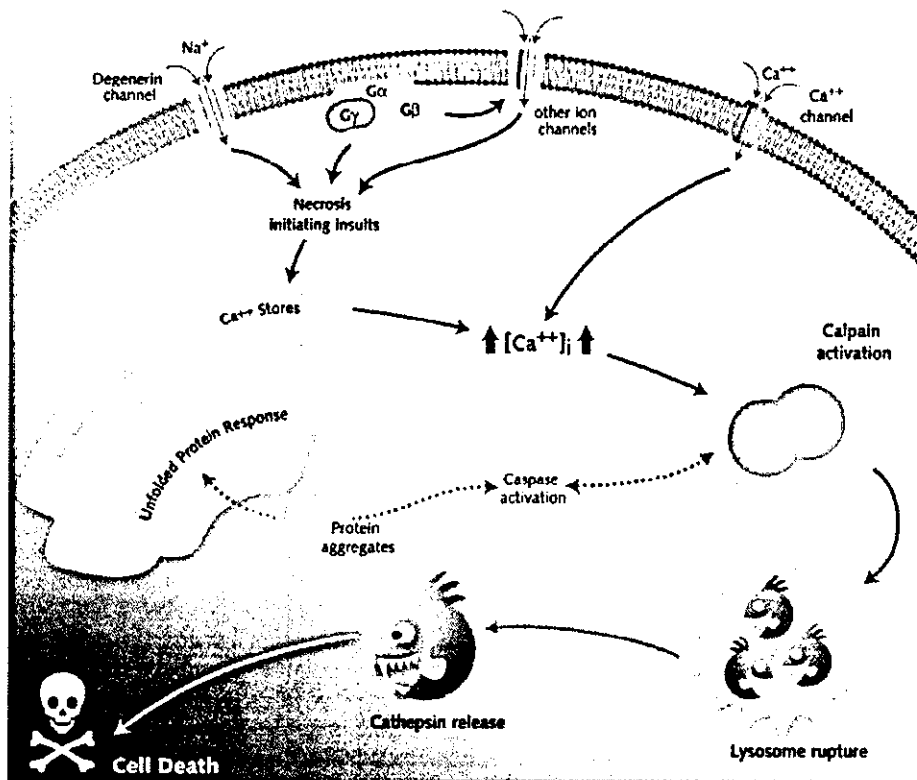
Fig. 4. Calcium-induced calpain–cathepsin cascade as a mechanism of ischemic neuronal death ('calpain–cathepsin hypothesis' formulated in [33]). The necrosis initiating insults may provoke intracellular Ca^{2+} mobilization through uptake of extracellular Ca^{2+} and/or release from internal stores. Ca^{2+} mobilization subsequently induces lysosomal rupture presumably with the aid of reactive oxygen species. The released cathepsin proteases degrade cell constitutive proteins leading to the neuronal death (cited from EMBO Rep. 3 (2002) 604–609).

sic concept of the calpain–cathepsin hypothesis, originally proposed for the monkey experimental paradigm [33].

5. Cross-talks between apoptosis and necrosis, and between ischemia and Alzheimer

The postischemic neuronal death may involve a combination of apoptotic and necrotic processes even at the level of the individual neuron [12,82,83]. Although paradoxically, it is likely that caspase-mediated proteolysis contributes to neuronal necrosis by the cleavage and inactivation of the plasma membrane Ca^{2+} pump [84]. This, in turn, disrupts intracellular Ca^{2+} homeostasis with the resultant Ca^{2+} overload, and further stimulates the calpain–cathepsin cascade through the sustained calpain activation [19]. Cleavage of the calpain inhibitor, calpastain by caspase-3 [85] might also stimulate calpain activation. Furthermore, cathepsins have been reported to activate caspase-3, either directly or indirectly [28,86]. Then, it is possible that caspases can be inappropriately activated, and participate to the initial phases of necrotic cascade, being isolated from the final phase of the apoptotic cascade. Accordingly, neither any discernible apoptotic morphology nor DNA ladder were seen in the postischemic CA1 neurons of monkeys despite cleavage and translocation of CAD [18,19].

Interestingly, in the pathogenesis of Alzheimer's disease, several reports pointed to an important role of calpains [87–92]. Widespread activation of μ-calpain in the Alzheimer brain has been demonstrated previously by biochemical methods [89]. Taniguchi et al. [91] analyzed expression of activated μ-calpain in human brain extracts by comparing eight Alzheimer patients (M:F = 2:6, mean 82 years old) with nine age-matched controls (M:F = 5:4, mean 77 years old). Intense bands of activated μ-calpain were consistently seen in the Alzheimer brain. Further, the band intensities of activated μ-calpain were about sevenfold ($P < 0.05$) in the Alzheimer brains compared to the control brains (Fig. 5) [91]. Previous studies showed that the populations of degenerating neurons in Alzheimer's disease exhibit robust up-regulation of the lysosomal system [92]. Then, it is probable that the calpain-mediated lysosomal spillage of hydrolytic enzymes might occur also in the Alzheimer neurons, and can explain the mechanisms of neuronal degeneration in Alzheimer's disease. It is probable that the mechanism of necrotic neuronal death should be conserved in spite of the diversity of pathologic conditions that initiate cell death.

1-9: Control, 10-17: Alzheimer
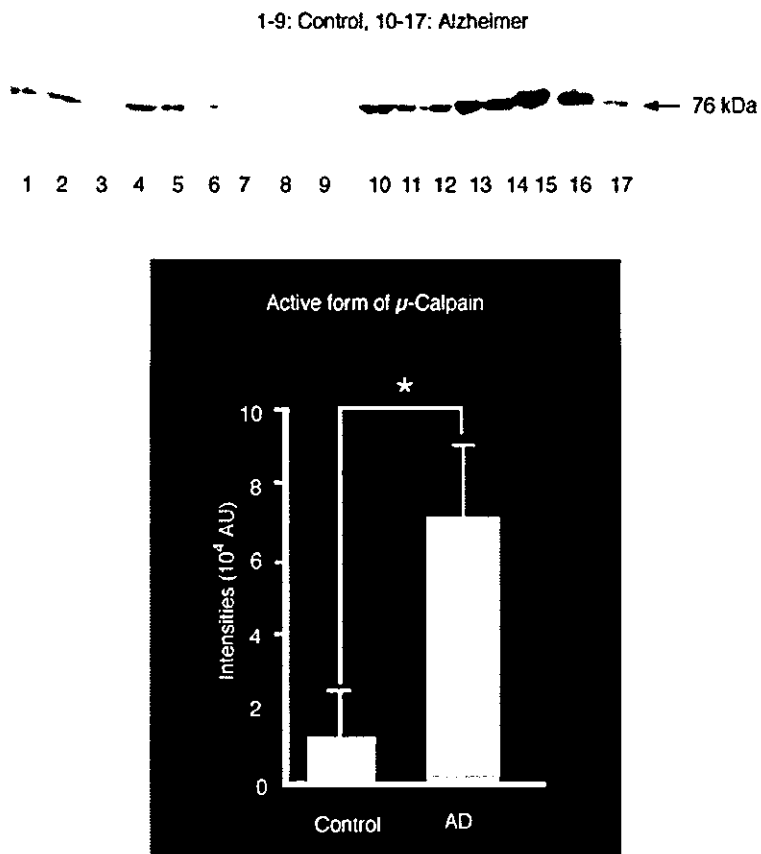

1 2 3 4 5 6 7 8 9   10 11 12 13 14 15 16 17

Fig. 5. Expression of activated μ-calpain in human brain extracts by comparing eight (10–17) Alzheimer patients with nine (1–9) age-matched controls. Intense bands of activated μ-calpain were consistently seen in the Alzheimer brain (upper), and its band intensities (AD) were about seven-fold ($^*P < 0.05$) compared to the control brains (lower) (cited from [91]).

6. Conclusion

Now, it is becoming widely accepted that the lysosomal system emerges as one of the main players during the final stage of neuronal necrosis. Spillage of hydrolytic enzymes from lysosomes into the cytoplasm due to the activated μ-calpain-mediated lysosomal membrane disruption, presumably with the aid of reactive oxygen species, executes neuronal necrosis or degeneration from C. elegans to primates.

Uncited references

[79,80].

References

[1] S.A. Lipton, P. Nicotera, Calcium, free radicals and excitotoxins in neuronal apoptosis, Cell Calcium 23 (1998) 165–171.

[2] M.P. Mattson, Apoptosis in neurodegenerative disorders, Nat. Rev. Mol. Cell Biol. 1 (2000) 120–129.

[3] R. Sattler, M. Tymianski, Molecular mechanisms of calcium-dependent excitotoxicity, J. Mol. Med. 78 (2000) 3–13.

[4] K. Xu, N. Tavernarakis, M. Driscoll, Necrotic cell death in C. elegans requires the function of calreticulin and regulators of Ca(2+) release from the endoplasmic reticulum, Neuron 31 (2001) 957–971.

[5] C. De Duve, R. Wattiaux, Functions of lysosomes, Annu. Rev. Physiol. 28 (1966) 435–492.

[6] M.M. Metzstein, G.M. Stanfield, H.R. Horvitz, Genetics of programmed cell death in C. elegans: past, present and future, Trends Genet. 14 (1998) 410–416.

[7] P. Meier, A. Finch, G. Evan, Apoptosis in development, Nature 407 (2000) 796–801.

[8] J.C. Ameisen, On the origin, evolution, and nature of programmed cell death: a timeline of four billion years, Cell Death Differ. 9 (2002) 367–393.

[9] J.F. Kerr, A.H. Wyllie, A.R. Currie, Apoptosis: a basic biological phenomenon with wide-ranging implications in tissue kinetics, Br. J. Cancer 26 (1972) 239–257.

[10] A.H. Wyllie, J.F. Kerr, A.R. Currie, Cell death: the significance of apoptosis, Int. Rev. Cytol. 68 (1980) 251–306.

[11] G. Majno, I. Joris, Apoptosis, oncosis, and necrosis. An overview of cell death, Am. J. Pathol. 146 (1995) 3–15.

[12] L.J. Martin, N.A. Al-Abdulla, A.M. Brambrink, J.R. Kirsch, F.E. Sieber, C. Portera-Cailliau, Neurodegeneration in excitotoxicity, global cerebral ischemia, and target deprivation: a perspective on the contributions of apoptosis and necrosis, Brain Res. Bull. 46 (1998) 281–309.

[13] L.J. Martin, Neuronal cell death in nervous system development, disease, and injury (review), Int. J. Mol. Med. 7 (2001) 455–478.

[14] M. Los, S. Wesselborg, K. Schulze-Osthoff, The role of caspases in development, immunity, and apoptotic signal transduction: lessons from knockout mice, Immunity 10 (1999) 629–639.

[15] M. Leist, M. Jaattela, Four deaths and a funeral: from caspases to alternative mechanisms, Nat. Rev. Mol. Cell Biol. 2 (2001) 589–598.

[16] M. Turmaine, A. Raza, A. Mahal, L. Mangiarini, G.P. Bates, S.W. Davies, Nonapoptotic neurodegeneration in a transgenic mouse model of Huntington's disease, Proc. Natl. Acad. Sci. U.S.A. 97 (2000) 8093–8097.

[17] S. Sperandio, I. de Belle, D.E. Bredesen, An alternative, nonapoptotic form of programmed cell death, Proc. Natl. Acad. Sci. U.S.A. 97 (2000) 14376–14381.

[18] T. Tsukada, M. Watanabe, T. Yamashima, Implications of CAD and DNase II in ischemic neuronal necrosis specific for the primate hippocampus, J. Neurochem. 79 (2001) 1196–1206.

[19] T. Yamashima, A.B. Tonchev, T. Tsukada, M. Tada, T.C. Saido, S. Imajoh-Ohmi, T. Momoi, E. Kominami, Sustained calpain activation associated with lysosomal rupture executes necrosis of the postischemic CA1 neurons in primates, Hippocampus (in press).

[20] D.G. Fujikawa, Confusion between neuronal apoptosis and activation of programmed cell death mechanisms in acute necrotic insults, Trends Neurosci. 23 (2000) 410–411.

[21] M. Roy, R. Sapolsky, Neuronal apoptosis in acute necrotic insults: why is this subject such a mess? Trends Neurosci. 22 (1999) 419–422.

[22] A. Boveris, B. Chance, The mitochondrial generation of hydrogen peroxide. General properties and effect of hyperbaric oxygen, Biochem. J. 134 (1973) 707–716.

[23] H.A. Kontos, E. George, Brown memorial lecture. Oxygen radicals in cerebral vascular injury, Circ. Res. 57 (1985) 508–516.

[24] J.T. Coyle, P. Puttfarcken, Oxidative stress, glutamate, and neurodegenerative disorders, Science 262 (1993) 689–695.

[25] P.H. Chan, Role of oxidants in ischemic brain damage, Stroke 27 (1996) 1124–1129.

[26] P. Nicotera, S.A. Lipton, Excitotoxins in neuronal apoptosis and necrosis, J. Cereb. Blood Flow Metab. 19 (1999) 583–591.

[27] S. Lankiewicz, C. Marc Luetjens, N. Truc Bui, A.J. Krohn, M. Poppe, G.M. Cole, T.C. Saido, J.H. Prehn, Activation of calpain I converts excitotoxic neuron death into a caspase-independent cell death, J. Biol. Chem. 275 (2000) 17064–17071.

[28] T. Yamashima, Implication of cysteine proteases calpain, cathepsin and caspase in ischemic neuronal death of primates, Prog. Neurobiol. 62 (2000) 273–295.

[29] T. Yamashima, T.C. Saido, M. Takita, A. Miyazawa, J. Yamano, A. Miyakawa, H. Nishijyo, J. Yamashita, S. Kawashima, T. Ono, T. Yoshioka, Transient brain ischaemia provokes Ca^{2+}, PIP_2 and calpain responses prior to delayed neuronal death in monkeys, Eur. J. Neurosci. 8 (1996) 1932–1944.

[30] L. Zhao, T. Yamashima, X.D. Wang, A.B. Tonchev, J. Yamashita, T. Kakiuchi, S. Nishiyama, S. Kuhara, K. Takahashi, H. Tsukada, PET imaging of ischemic neuronal death of living monkeys, Hippocampus 12 (2002) 109–118.

[31] M. Yoshida, T. Yamashima, L. Zhao, K. Tsuchiya, Y. Kohda, A.B. Tonchev, M. Matsuda, E. Kominami, Primate neurons show different vulnerability to transient ischemia and response to cathepsin inhibition, Acta Neuropathol. (Berl.) 104 (2002) 267–272.

[32] P. Syntichaki, K. Xu, M. Driscoll, Specific aspartyl and calpain proteases are required for neurodegeneration in *C. elegans*, Nature 419 (2002) 939–944.

[33] T. Yamashima, Y. Kohda, K. Tsuchiya, T. Ueno, J. Yamashita, T. Yoshioka, E. Kominami, Inhibition of ischaemic hippocampal neuronal death in primates with catepsin B inhibitor CA-074: a novel strategy for neuroprotection based on 'calpain-cathepsin hypothesis', Eur. J. Neurosci. 10 (1998) 1723–1733.

[34] C. Charriaut-Marlangue, Y. Ben-Ari, A cautionary note on the use of the TUNEL stain to determine apoptosis, Neuroreport 7 (1995) 61–64.

[35] F. Mangili, C. Cigala, G. Santambrogio, Staining apoptosis in paraffin sections. Advantages and limits, Anal. Quant. Cytol. Histol. 21 (1999) 273–276.

[36] C. Stadelmann, H. Lassmann, Detection of apoptosis in tissue sections, Cell Tissue Res. 301 (2000) 19–31.

[37] G.M. Cohen, Caspases: the executioners of apoptosis, Biochem. J. 326 (Pt. 1) (1997) 1–16.

[38] W.C. Earnshaw, L.M. Martins, S.H. Kaufmann, Mammalian caspases: structure, activation, substrates, and functions during apoptosis, Annu. Rev. Biochem. 68 (1999) 383–424.

[39] M.O. Hengartner, The biochemistry of apoptosis, Nature 407 (2000) 770–776.

[40] A. Strasser, L. O'Connor, V.M. Dixit, Apoptosis signaling, Annu. Rev. Biochem. 69 (2000) 217–245.

[41] S.H. Kaufmann, M.O. Hengartner, Programmed cell death: alive and well in the new millennium, Trends Cell Biol. 11 (2001) 526–534.

[42] D.W. Nicholson, N.A. Thornberry, Caspases: killer proteases, Trends Biochem. Sci. 22 (1997) 299–306.

[43] K. Kuida, T.S. Zheng, S. Na, C. Kuan, D. Yang, H. Karasuyama, P. Rakic, R.A. Flavell, Decreased apoptosis in the brain and premature lethality in CPP32-deficient mice, Nature 384 (1996) 368–372.

[44] J. Chen, T. Nagayama, K. Jin, R.A. Stetler, R.L. Zhu, S.H. Graham, R.P. Simon, Induction of caspase-3-like protease may mediate delayed neuronal death in the hippocampus after transient cerebral ischemia, J. Neurosci. 18 (1998) 4914–4928.

[45] X. Liu, H. Zou, C. Slaughter, X. Wang, DFF, a heterodimeric protein that functions downstream of caspase-3 to trigger DNA fragmentation during apoptosis, Cell 89 (1997) 175–184.

[46] M. Enari, H. Sakahira, H. Yokoyama, K. Okawa, A. Iwamatsu, S. Nagata, A caspase-activated DNase that degrades DNA during apoptosis, and its inhibitor ICAD, Nature 391 (1998) 43–50.

[47] H. Sakahira, M. Enari, S. Nagata, Cleavage of CAD inhibitor in CAD activation and DNA degradation during apoptosis, Nature 391 (1998) 96–99;
H. Sakahira, M. Enari, S. Nagata, Excitotoxicity, J. Mol. Med. 78 (2000) 3–13.

[48] N. Mukae, M. Enari, H. Sakahira, Y. Fukuda, J. Inazawa, H. Toh, S. Nagata, Molecular cloning and characterization of human caspase-activated DNase, Proc. Natl. Acad. Sci. U.S.A. 95 (1998) 9123–9128.

[49] G. Cao, W. Pei, J. Lan, R.A. Stetler, Y. Luo, T. Nagayama, S.H. Graham, X.M. Yin, R.P. Simon, J. Chen, Caspase-activated DNase/DNA fragmentation factor 40 mediates apoptotic DNA fragmentation in transient cerebral ischemia and in neuronal cultures, J. Neurosci. 21 (2001) 4678–4690.

[50] T.C. Saido, H. Sorimachi, K. Suzuki, Calpain: new perspectives in molecular diversity and physiological-pathological involvement, FASEB J. 8 (1994) 814–822.

[51] K. Suzuki, H. Sorimachi, T. Yoshizawa, K. Kinbara, S. Ishiura, Calpain: novel family members, activation, and physiologic function, Biol. Chem. Hoppe Seyler 376 (1995) 523–529.

[52] E. Melloni, M. Michetti, F. Salamino, R. Minafra, S. Pontremoli, Modulation of the calpain autoproteolysis by calpastatin and phospholipids, Biochem. Biophys. Res. Commun. 229 (1996) 193–197.

[53] S.K. Ray, M. Fidan, M.W. Nowak, G.G. Wilford, E.L. Hogan, N.L. Banik, Oxidative stress and Ca^{2+} influx upregulate calpain and induce apoptosis in PC12 cells, Brain Res. 852 (2000) 326–334.

[54] S. Schoonbroodt, V. Ferreira, M. Best-Belpomme, J.R. Boelaert, S. Legrand-Poels, M. Korner, J. Piette, Crucial role of the amino-terminal tyrosine residue 42 and the carboxyl-terminal PEST domain of I kappa B alpha in NF-kappa B activation by an oxidative stress, J. Immunol. 164 (2000) 4292–4300.

[55] S.K. Ray, G.G. Wilford, C.V. Crosby, E.L. Hogan, N.L. Banik, Diverse stimuli induce calpain overexpression and apoptosis in C6 glioma cells, Brain Res. 829 (1999) 18–27.

[56] M. Andersson, J. Sjostrand, A. Petersen, J.O. Karlsson, Calcium-dependent proteolysis in rabbit lens epithelium after oxidative stress, Ophthalmic Res. 30 (1998) 157–167.

614 [57] K. Kinbara, S. Ishiura, S. Tomioka, H. Sorimachi, S.Y. Jeong, S.
615   Amano, H. Kawasaki, B. Kolmerer, S. Kimura, S. Labeit, K. Suzuki,
616   Purification of native p94, a muscle-specific calpain, and character-
617   ization of its autolysis, Biochem. J. 335 (Pt 3) (1998) 589–596.
618 [58] M.S. Lee, Y.T. Kwon, M. Li, J. Peng, R.M. Friedlander, L.H. Tsai,
619   Neurotoxicity induces cleavage of p35 to p25 by calpain, Nature 405
620   (2000) 360–364.
621 [59] A. Mouatt-Prigent, J.O. Karlsson, Y. Agid, E.C. Hirsch, Increased M-
622   calpain expression in the mesencephalon of patients with Parkinson's
623   disease but not in other neurodegenerative disorders involving the
624   mesencephalon: a role in nerve cell death? Neuroscience 73 (1996)
625   979–987.
626 [60] K. Takahashi, Intracellular calcium-dependent proteolysis, in: R.L.
627   Mellgren, T. Murachi (Eds.), Calpain Substrate Specificity, CRC
628   Press, Boca Raton, 1990, pp. 55–74 (Chapter 4).
629 [61] S. Fahn, G. Cohen, The oxidant stress hypothesis in Parkinson's
630   disease: evidence supporting it, Ann. Neurol. 32 (1992) 804–812.
631 [62] C. Behl, B. Moosmann, Oxidative nerve cell death in Alzheimer's
632   disease and stroke: antioxidants as neuroprotective compounds, Biol.
633   Chem. 383 (2002) 521–536.
634 [63] J.W. Putney Jr., Excitement about calcium signaling in inexcitable
635   cells, Science 262 (1993) 676–678.
636 [64] A. Ghosh, M.E. Greenberg, Calcium signaling in neurons: molecular
637   mechanisms and cellular consequences, Science 268 (1995) 239–247.
638 [65] U.T. Brunk, H. Dalen, K. Roberg, H.B. Hellquist, Photo-oxidative
639   disruption of lysosomal membranes causes apoptosis of cultured
640   human fibroblasts, Free. Radic. Biol. Med. 23 (1997) 616–626.
641 [66] N. Brachfeld, Bioenergetics of the normal and anoxic myocardium,
642   Adv. Cardiopulm. Dis. 4 (1969) 66–90.
643 [67] K. Ichihara, T. Haneda, S. Onodera, Y. Abiko, Inhibition of ischemia-
644   induced subcellular redistribution of lysosomal enzymes in the per-
645   fused rat heart by the calcium entry blocker, diltiazem, J. Pharmacol.
646   Exp. Ther. 242 (1987) 1109–1113.
647 [68] L.V. Molchanova, S.E. Nickulina, T.N. Ivanova, A.I. Ivanov, E.D.
648   Polyskova, Role of cAMP in regulation of activity of acid hydro-
649   lases of rat heart and liver during ischemia and after recirculation,
650   Resuscitation 22 (1991) 261–274.
651 [69] B.C. White, A. Daya, D.J. De Gracia, B.J. O'Neil, J.M. Skjaerlund,
652   S. Trumble, G.S. Krause, J.A. Rafols, Florescent histochemical lo-
653   calization of lipid peroxidation during brain reperfusion following
654   cardiac arrest, Acta Neuropathol. (Berl.) 86 (1993) 1–9.
655 [70] E. Adamec, P.S. Mohan, A.M. Cataldo, J.P. Vonsattel, R.A. Nixon,
656   Up-regulation of the lysosomal system in experimental models of
657   neuronal injury: implications for Alzheimer's disease, Neuroscience
658   100 (2000) 663–675.
659 [71] M. Murata, S. Miyashita, C. Yokoo, M. Tamai, K. Hanada, K.
660   Hatayama, T. Towatari, T. Nikawa, N. Katunuma, Novel epoxysuc-
661   cinyl peptides. Selective inhibitors of cathepsin B, in vitro, FEBS
662   Lett. 280 (1991) 307–310.
663 [72] T. Towatari, T. Nikawa, M. Murata, C. Yokoo, M. Tamai, K. Hanada,
664   N. Katunuma, Novel epoxysuccinyl peptides. A selective inhibitor
665   of cathepsin B, in vivo, FEBS Lett. 280 (1991) 311–315.
666 [73] S. Hashida, T. Towatari, E. Kominami, N. Katunuma, Inhibitions by
667   E-64 derivatives of rat liver cathepsin B and cathepsin L in vitro
668   and in vivo, J. Biochem. (Tokyo) 88 (1980) 1805–1811.
669 [74] S. Hashida, E. Kominami, N. Katunuma, Inhibitions of cathepsin B
670   and cathepsin L by E-64 in vivo. II. Incorporation of [3H]E-64 into
671   rat liver lysosomes in vivo, J. Biochem. (Tokyo) 91 (1982) 1373–
672   1380.
673 [75] N. Katunuma, E. Kominami, Structure, properties, mechanisms, and
674   assays of cysteine protease inhibitors: cystatins and E-64 derivatives,
675   Methods Enzymol. 251 (1995) 382–397.

676 [76] J. Gray, M.M. Haran, K. Schneider, S. Vesce, A.M. Ray, D.
677   Owen, I.R. White, P. Cutler, J.B. Davis, Evidence that inhibition of
678   cathepsin-B contributes to the neuroprotective properties of caspase
679   inhibitor Tyr-Val-Ala-Asp-chloromethyl ketone, J. Biol. Chem. 276
680   (2001) 32750–32755.
681 [77] C. de Duve, Lysosomes revisited, Eur. J. Biochem. 137 (1983) 391–
682   397.
683 [78] Y. Kitao, K. Ozawa, M. Miyazaki, M. Tamatani, T. Kobayashi,
684   H. Yanagi, M. Okabe, M. Ikawa, T. Yamashima, D.M. Stern, O.
685   Hori, S. Ogawa, Expression of the endoplasmic reticulum molecular
686   chaperone (ORP150) rescues hippocampal neurons from glutamate
687   toxicity, J. Clin. Invest. 108 (2001) 1439–1450.
688 [79] L.R. Roberts, H. Kurosawa, S.F. Bronk, P.J. Fesmier, L.B. Agellon,
689   W.Y. Leung, F. Mao, G.J. Gores, Cathepsin B contributes to bile salt-
690   induced apoptosis of rat hepatocytes, Gastroenterology 113 (1997)
691   1714–1726.
692 [80] M.E. Guicciardi, H. Miyoshi, S.F. Bronk, G.L. Gores, Cathepsin B
693   knockout mice are resistant to tumor necrosis factor-alpha-mediated
694   hepatocyte apoptosis and liver injury: implications for therapeutic
695   applications, Am. J. Pathol. 159 (2001) 2045–2054.
696 [81] L. Foghsgaard, D. Wissing, D. Mauch, U. Lademann, L. Bastholm,
697   M. Boes, F. Elling, M. Leist, M. Jaattela, Cathepsin B acts as a
698   dominant execution protease in tumor cell apoptosis induced by
699   tumor necrosis factor, J. Cell Biol. 153 (2001) 999–1010.
700 [82] J.N. Davis, F.J. Antonawich, Role of apoptotic proteins in is-
701   chemic hippocampal damage, Ann. N.Y. Acad. Sci. 835 (1997) 309–
702   320.
703 [83] J.P. MacManus, A.M. Buchan, Apoptosis after experimental stroke:
704   fact or fashion? J. Neurotrauma. 10 (2000) 899–914.
705 [84] B.L. Schwab, D. Guerini, C. Didszun, D. Bano, E. Ferrando-May, E.
706   Fava, J. Tam, D. Xu, S. Xanthoudakis, D.W. Nicholson, E. Carafoli, P.
707   Nicotera, Cleavage of plasma membrane calcium pumps by caspases:
708   a link between apoptosis and necrosis, Cell Death Differ. 9 (2002)
709   818–831.
710 [85] M.I. Pom-Ares, A. Samali, S. Orrenius, Cleavage of the calpain
711   inhibitor, calpastatin, during apoptosis, Cell Death Differ. 5 (1998)
712   1028–1033.
713 [86] K.F. Ferri, G. Kroemer, Organelle-specific initiation of cell death
714   pathways, Nat. Cell Biol. 3 (2001) E255–E263.
715 [87] N. Iwamoto, W. Thangnipon, C. Crawford, P.C. Emson, Localization
716   of calpain immunoreactivity in senile plaques and in neurones un-
717   dergoing neurofibrillary degeneration in Alzheimer's disease, Brain
718   Res. 561 (1991) 177–180.
719 [88] S. Shimohama, T. Suenaga, W. Araki, Y. Yamaoaka, K. Shimizu, J.
720   Kimura, Presence of calpain II immunoreactivity in senile plaques
721   in Alzheimer's disease, Brain Res. 558 (1991) 105–108.
722 [89] K.I. Saito, J.S. Elce, J.E. Hamos, R.A. Nixon, Widespread activa-
723   tion of calcium-activated neutral proteinase calpain in the brain in
724   Alzheimer disease: a potential molecular basis for neuronal degen-
725   eration, Proc. Natl. Acad. Sci. U.S.A. 90 (1993) 2628–2632.
726 [90] R.A. Nixon, K.I. Saito, F. Grynspan, W.R. Griffin, S. Katayama,
727   T. Honda, P.S. Mohan, T.B. Shea, M. Beermann, Calcium-activated
728   neutral proteinase calpain system in aging and Alzheimer disease,
729   Ann. NY Acad. Sci. 747 (1994) 77–91.
730 [91] S. Taniguchi, Y. Fujita, S. Hayashi, A. Kakita, H. Takahashi, S.
731   Murayama, T.C. Saido, S. Hisanaga, T. Iwatsubo, M. Hasegawa,
732   Calpain-mediated degradation of p35 to p25 in postmortem human
733   and rat brains, FEBS Lett. 489 (2001) 46–50.
734 [92] E. Adamec, P. Mohan, J.P. Vonsattel, R.A. Nixon, Calpain activation
735   in neurodegenerative diseases: confocal immunofluorescence study
736   with antibodies specifically recognizing the active form of calpain
737   2, Acta Neuropathol. (Berl.) 104 (2002) 92–104.

The influence of age on apoptotic and other mechanisms of cell death after cerebral hypoxia–ischemia

C Zhu[*,1,2], X Wang[1,2], F Xu[1,2], BA Bahr[3], M Shibata[4], Y Uchiyama[4], H Hagberg[1,5] and K Blomgren[1,6]

[1] Department of Physiology, Göteborg University, Göteborg, Sweden
[2] Department of Pediatrics, The Third Affiliated Hospital of Zhengzhou University, Zhengzhou, PR, China
[3] Department of Pharmaceutical Sciences and the Neurosciences Program, University of Connecticut, Storrs, CT, USA
[4] Department of Cell Biology and Neuroscience, Osaka University Graduate School of Medicine, Osaka, Japan
[5] Department of Obstetrics and Gynecology, Sahlgrenska University Hospital, Göteborg, Sweden
[6] Department of Pediatrics, The Queen Silvia Children's Hospital, Göteborg, Sweden
[*] Corresponding author: C Zhu, Department of Physiology, Perinatal Center, Göteborg University, Box 432, SE 405 30 Göteborg, Sweden. Tel: +46 31 773 3539; Fax: +46 31 773 3512; E-mail: changlian.zhu@fysiologi.gu.se

Abstract

Q1
Unilateral hypoxia–ischemia (HI) was induced in C57/BL6 male mice on postnatal day (P) 5, 9, 21 and 60, corresponding developmentally to premature, term, juvenile and adult human brains, respectively. HI duration was adjusted to obtain a similar extent of brain injury at all ages. Apoptotic mechanisms (nuclear translocation of apoptosis-inducing factor, cytochrome c release and caspase-3 activation) were several-fold more pronounced in immature than in juvenile and adult brains. Necrosis-related calpain activation was similar at all ages. The CA1 subfield shifted from apoptosis-related neuronal death at P5 and P9 to necrosis-related calpain activation at P21 and P60. Oxidative stress (nitrotyrosine formation) was also similar at all ages. Autophagy, as judged by the autophagosome-related marker LC-3 II, was more pronounced in adult brains. To our knowledge, this is the first report demonstrating developmental regulation of AIF-mediated cell death as well as involvement of autophagy in a model of brain injury.
Cell Death and Differentiation (2004) 0, 000–000. doi:10.1038/sj.cdd.4401545

Introduction

The extent of hypoxic–ischemic (HI) injury depends on the degree of maturation of the brain as well as on the severity and duration of the insult.[1–7] It is generally accepted that neurons in the immature brain tolerate a longer period of oxygen deprivation and/or ischemia than those in the adult brain.[1,3] However, there are conflicting reports, showing that the immature brain is less resistant to HI brain damage than its adult counterpart.[4] This is supported by other studies after HI or excitotoxic injury.[8,9] Furthermore, clinical data suggest that outcome and mortality after acute brain injury are age dependent, with more severe injuries in infants than in adults.[8,10]

Cell death is usually classified as apoptotic or necrotic based on biochemical and morphological criteria,[11,12] even though recent data suggest that mixed morphological phenotypes are frequently observed after ischemic insults.[12–14] Necrotic cell death is a pathological process resulting from tissue damage and loss of energy. Apoptosis is a genetically controlled cell death that was initially recognized for its role in development. In some brain regions, more than half of the neurons die by apoptosis during brain development.[15] Many apoptosis-related factors have been demonstrated to be upregulated in the immature brain, such as caspase-3, Apaf-1, Bcl-2 and Bax.[16–19] Activation of apoptotic mechanisms contributes to the pathogenesis of brain damage in acute neuropathological disorders, such as HI, particularly in the immature brain.[1,14,16,20–25] Autophagy is another type of cell death mechanism with distinct morphological features whereby lysosome-mediated engulfment of injured cells or cellular fragments can occur.[26] It seems clear that, depending on the developmental level of the brain at the time of injury, different cell types and regions will be injured, at different rates, and different mechanisms of injury will be activated.[1,3,22,27,28] Understanding the nature of cell death after HI at different developmental stages is essential to be able to choose effective therapeutic targets,[29,30] and since these vary during development, prevention and treatment of brain injury need to be adjusted accordingly. To better understand the pathogenesis and developmental variations of HI neuronal cell death, we developed a mouse model where a similar extent of injury could be achieved by adjusting the duration of the hypoxia time, thereby enabling us to study the relative contribution of different mechanisms at different ages. Specifically, we investigated caspase-dependent and caspase-independent apoptotic mechanisms as well as one

marker of oxidative stress (NOS-dependent, peroxynitrite-mediated nitrotyrosine formation), necrosis-related activation of calpains and autophagy.

Results

HI brain injury

Similar tissue injury was seen in the cortex, striatum, hippocampus and thalamus in the ipsilateral hemisphere at all ages (Figure 1a). The nucleus habenularis (NH), however displayed a marked developmental change in its susceptibility to HI. The NH is very sensitive to HI in the immature brain,[31] but this vulnerability decreased with age and the NH was resistant to HI in P60 mice (Figure 1b).The neuropathological score and tissue loss were virtually identical at P5, P9, P21 and P60 using the different durations of hypoxic exposure indicated in Materials and Methods (Figure 1c).

Apoptosis-inducing factor (AIF) translocation and cytochrome *c* (Cyt *c*) release from mitochondria after HI

The levels of AIF protein in mouse brain homogenates were virtually unchanged during normal brain development from P5 to P60 (Figure 2a). In the mitochondrial fraction, there was about 20% less AIF in the ipsilateral hemisphere compared with the contralateral hemisphere in P5 mice 24 h post-HI, indicating that this amount had been released. This AIF release was reduced to about 10% in juvenile and adult brains (Figure 2b). In tissue sections, AIF immunoreactivity was non-nuclear in normal neurons; however, in damaged brain areas, as judged by the loss of MAP-2, AIF was translocated from mitochondria to nuclei very early after HI, producing a distinct nuclear staining (Figure 2c), in agreement with our earlier findings in the neonatal rat brain after HI,[32] in the adult mouse brain after focal ischemia[33] and in progenitor cells of the developing brain after irradiation.[34] The number of AIF-positive nuclei increased significantly at 3 h post-HI and reached a peak at 24 h after the insult in most regions of the immature brain, more pronounced in P5 mice (Figure 3). Significant, but much fewer, AIF-positive nuclei were observed in the mature mouse brain regions (except for the
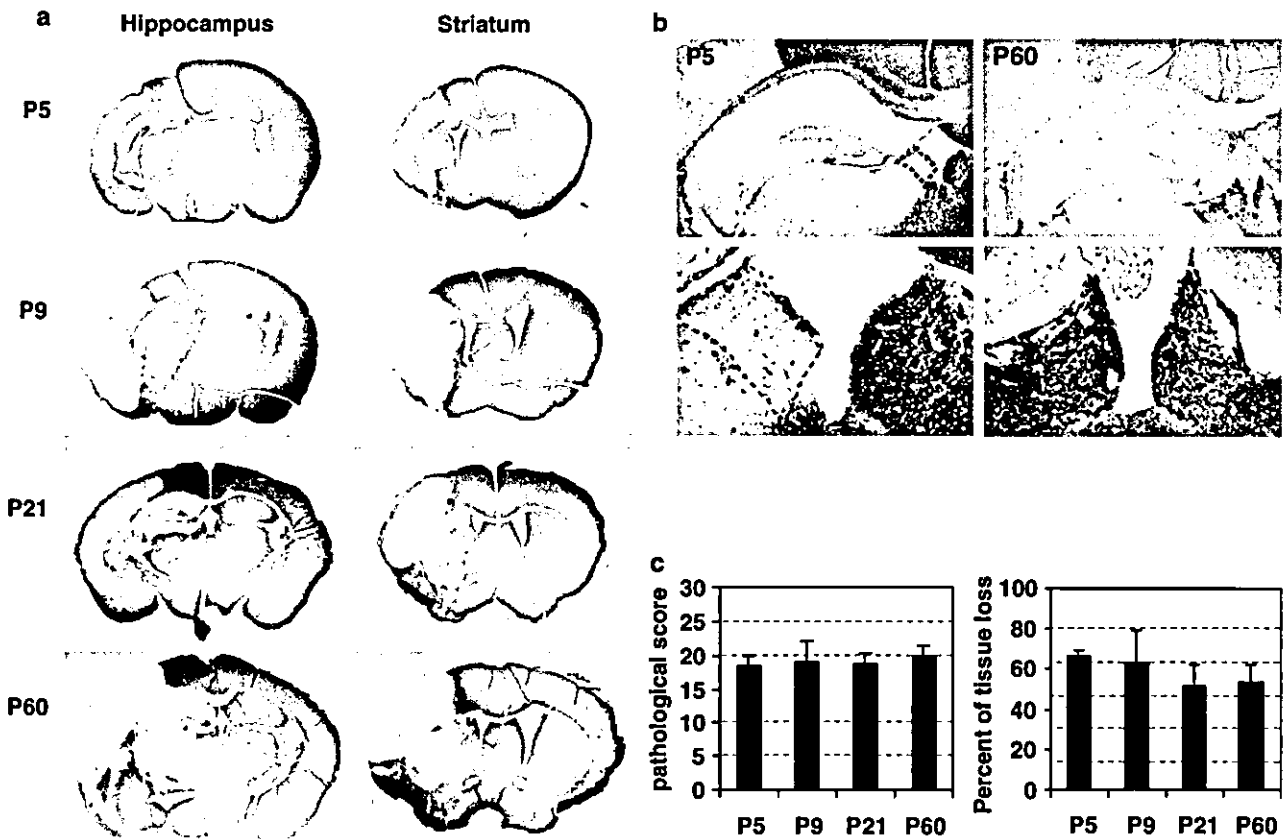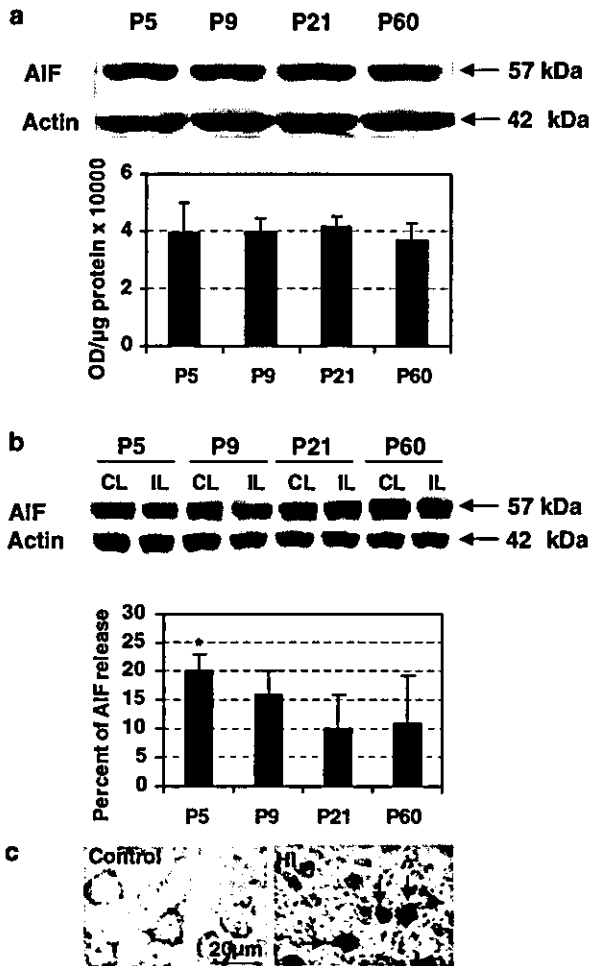

Figure 1 Brain injury after HI in the developing brain. (a) Representative MAP-2 staining 72 h after HI at the dorsal hippocampus and striatum levels of P5, P9, P21 and P60 mice after 65, 60, 50 and 40 min hypoxia, respectively. The injury encompassed large areas of the cortex, hippocampus, striatum and thalamus. (b) The sensitivity of the NH to HI was very different in the immature (P5) brain and adult (P60) brains. This area is very vulnerable in P5 brains but there was no obvious injury in the adult brains as indicated by MAP-2 staining 24 h post-HI. The dotted areas are shown in a larger magnification in the lower panels. (c) The brain injury was similar between different age groups as evaluated by the pathological score (left graph) and tissue loss (right graph) ($n = 6$ for each age group)

a

P5   P9   P21   P60

AIF ← 57 kDa

Actin ← 42 kDa

b

P5   P9   P21   P60

CL IL CL IL CL IL CL IL

AIF ← 57 kDa

Actin ← 42 kDa

c

Control

Figure 2   Developmental regulation of AIF. (a) Immunoblots of normal brain homogenate samples from postnatal day (P) 5, 9, 21, 60 (n = 5 for each age), demonstrating that there was no significant change in the AIF protein levels during normal development. The actin staining on the same membrane verified equal loading. (b) AIF was released from the mitochondrial fraction in the ipsilateral (IL) compared with the contralateral (CL) hemispheres at 24 h post-HI. The loss of AIF was more pronounced in the immature brains (*P<0.05 compared with P21 and P60). The actin staining on the same membrane verified equal loading. (c) Typical AIF immunostaining of control and injured (HI) tissue. Injured cells displaying nuclear AIF staining are indicated by arrows. Bar = 20 μm

denate gyrus (DG)), especially in P60 mice. In the NH, the number of AIF-positive nuclei decreased dramatically with development reflecting the resistance to HI at P21 and P60 (Figure 3).

Another mitochondrial, proapoptotic protein, Cyt c, displayed an approximately two-fold increase during normal brain development (Figure 4a). It was released from mitochondria in the ipsilateral hemisphere after HI, more pronounced in the immature brain than in the adult brain (Figure 4b). In tissue sections, neuronal Cyt c staining was found to be more intense and distinct in the cytosol of damaged brain areas (Figure 4c), presumably indicating release of Cyt c from mitochondria, as demonstrated ear-

lier.[32,33] Counting of cells with strong cytoplasmic Cyt c staining, revealed a pattern similar to that of AIF-positive nuclei, with higher numbers in the immature brains, but the total number of strongly Cyt c staining cells was smaller than that of AIF-positive nuclei (Figure 5).

Caspase-3 activation after HI

Caspase-3, the most abundant effector caspase in the immature brain, decreased dramatically with brain maturation (Figure 6a), displaying an inverse correlation with Cyt c, as demonstrated earlier in the rat brain.[16,32] The 32 kDa proform was cleaved and produced the calpain-dependent 29 kDa and the caspase-dependent active 17 kDa fragments after HI in the ipsilateral hemisphere in the immature brains. The cleavage products were difficult to detect in the juvenile and adult brains (Figure 6b). Using an antibody against the 17 kDa active form of caspase-3 on tissue sections, conspicuous staining was obtained in numerous neurons in MAP-2-negative areas in the immature brains (Figure 6c), and this staining has earlier been shown to colocalize with other markers of cellular injury.[16,21,32] DEVDase assays showed that the caspase-3-like activity increased 31-fold in P5 and 25-fold in P9 mice 24 h post-HI, compared with the normal control brains (Figure 6b), consistent with when the peak of caspase-3 activation occurs in the neonatal rat brain after HI.[16,23] Caspase-3 activity increased about 40% in P21 and P60 mice, compared with the normal control brains (Figure 6d). Active caspase-3 staining in tissue sections increased at 3 h and reached a peak at 24 h post-HI in most regions in the immature and juvenile brains (P5, P9 and P21) (Figure 7). In the adult brains (P60), the caspase-3-positive cells appeared gradually and reached a peak at 72 h in all injured areas (Figure 7). The total number of active caspase-3-positive cells was lower in the juvenile and adult brains than in the immature brains, except for the CA3 (P21 and P60) and DG (P21) subfields of the hippocampus (Figure 7).

Calpain activation after HI

Calpain 1 did not change appreciably in the normal brains during development (Figure 8a), but after HI almost half of the calpain 1 was lost in the immature brains (Figure 8b), most likely as a result of activation and subsequent degradation.[35] In the juvenile and adult brains, however, the loss was significantly lower, only about 5% in P60 mice (Figure 8b). Calpain 2 was not significantly regulated during development, except for a somewhat higher level in P5 mice (Figure 8c). About 20–30% of the calpain 2 protein was lost after HI, but there was no significant difference between ages (Figure 8d). Activation of calpains results in specific fodrin cleavage products alpha-fodrin breakdown product (FBDP) of 145 and 150 kDa, relatively resistant to further degradation. FBDPs have been used extensively as markers of calpain activation, including after neonatal HI.[16,31,35–37] In this study, FBDPs were prominent after HI at all ages (Figure 8e), unlike the caspase-dependent 120 kDa cleavage product, which was apparent only in P5 and P9 mice (Figure 8e). In tissue sections, an antibody specific for the n-terminal 145 kDa FBDP, produced strong staining in injured neurons early after

Q2